



HAL
open science

The extravascular penetration of tirapazamine into tumours: a predictive model of the transport and efficacy of hypoxia specific cytotoxic analogues and the potential use of cucurbiturils to facilitate delivery

Clifford W Fong

► **To cite this version:**

Clifford W Fong. The extravascular penetration of tirapazamine into tumours: a predictive model of the transport and efficacy of hypoxia specific cytotoxic analogues and the potential use of cucurbiturils to facilitate delivery. *International journal of computational biology and drug design*, 2017, 10 (4), pp.343-372. 10.1504/IJCBDD.2017.10009055 . hal-01693232

HAL Id: hal-01693232

<https://hal.science/hal-01693232>

Submitted on 25 Jan 2018

HAL is a multi-disciplinary open access archive for the deposit and dissemination of scientific research documents, whether they are published or not. The documents may come from teaching and research institutions in France or abroad, or from public or private research centers.

L'archive ouverte pluridisciplinaire **HAL**, est destinée au dépôt et à la diffusion de documents scientifiques de niveau recherche, publiés ou non, émanant des établissements d'enseignement et de recherche français ou étrangers, des laboratoires publics ou privés.

The extravascular penetration of tirapazamine into tumours: a predictive model of the transport and efficacy of hypoxia specific cytotoxic analogues and the potential use of cucurbiturils to facilitate delivery.

Clifford W. Fong
Eigenenergy, Adelaide, South Australia.

Abstract

A multiparameter model of the diffusion, antiproliferative assays IC_{50} and aerobic and hypoxic clonogenic assays for a wide range of neutral and radical anion forms of tirapazamine (TPZ) analogues has found that: (a) extravascular diffusion is governed by the desolvation, lipophilicity, dipole moment and molecular volume, similar to passive and facilitated permeation through the blood brain barrier and other cellular membranes, (b) hypoxic assay properties of the TPZ analogues show dependencies on the electron affinity, as well as lipophilicity and dipole moment and desolvation, similar to other biological processes involving permeation of cellular membranes, including nuclear membranes, (c) aerobic properties are dependent on the almost exclusively on the electron affinity, consistent with electron transfer involving free radicals being dominant with little or no drug permeation of membranes, and most likely occurring in the extracellular matrix.

Application of the model to the DNA binding equilibrium constants of TPZ analogues with acridine or acridine-like moieties show that ligand water desolvation and lipophilicity are the dominant processes governing the DNA intercalation of TPZ analogues. This conclusion is consistent with DFT modelling of the complexes formed by TPZ analogues with neutral and N-protonated acridine moieties which intercalate with the guanine DNA nucleobases.

A quantum mechanical study has shown that TPZ can form stable complexes with cucurbit[7]uril as a precursor to proof of principle of improved TPZ delivery to tumours.

Keywords: Tirapazamine analogues, intra-tumoural diffusion, anti-cancer, hypoxia, cytotoxicity, DNA binding, cucurbiturils, quantum mechanics

Abbreviations

Tirapazamine TPZ, free energy of water desolvation $\Delta G_{\text{desolv,CDS}}$, lipophilicity free energy $\Delta G_{\text{lipo,CDS}}$, cavity dispersion solvent structure of the first solvation shell CDS, multicellular layers MCL, extracellular matrix ECM, diffusion through support membrane D_s , diffusion through multicellular layer D_{MCL} , cucurbit[n]urils CB, cucurbit[7]urils, CB[7], highest occupied molecular orbital HOMO, lowest unoccupied molecular orbital LUMO, density functional molecular orbital theory DFT, adiabatic electron affinity AEA, cisplatin CisPt, ratio aerobic property:hypoxic property HCR, aerobic aer, hypoxic hyp, DNA binding equilibrium constant K_{DNA} , multiple correlation coefficient R^2 , the F test of significance, standards errors for the estimate (SEE) and standard errors of the variables $SE(\Delta G_{\text{desolvCDS}})$, $SE(\Delta G_{\text{lipoCDS}})$, $SE(\text{Dipole Moment})$, $SE(\text{Molecular Volume})$, $SE(\text{AEA})$.

Contact: cwfong@internode.on.net

1. Introduction

Solid tumours have characteristic microenvironments as a result of poor vascular supply. The microenvironment consists of gradients of oxygen tension, cellular metabolites, nutrients, cell growth, and extracellular pH which vary in distance from the vascular supply network. Hypoxia is a characteristic of many cancers, and is a poor prognosis marker. Resistance to chemotherapy is strongly linked to hypoxia induced reduction in cell proliferation. Hypoxic regions of tumours are distant from vascular blood supply, making anti-cancer drug delivery a key factor in resistance induced by hypoxia. ¹⁻⁶ [Vaupel 2008-13, Tredan 2007, Minchinton 2006, Muz 2015]

Hypoxia is a common condition in a majority of malignant tumours and can lead to increased vascularisation and metastasis. When a tumour reaches to a critical size the nutrients diffusion is insufficient to supply the required amount of oxygen to the inner parts of the tumour resulting in hypoxia. The tumour microenvironment influences various cell signalling processes involved in tumour angiogenesis, metastasis, and development of the resistance to therapies. Hypoxia helps the tumour cells survive by giving them more aggressive phenotypes. The degree of hypoxia varies with tumour type and size. ⁶ [Muz 2015] Chemotherapy and radiotherapy treatment often encounter strong resistance from hypoxic regions inside the tumour. While there a negative correlation between the hypoxic fraction in tumours and the efficacy of radiotherapy and chemotherapies, there is also a correlation between the hypoxic fraction in tumours and cancer metastasis. ⁷ [Pettersen 2014]

Wardman 2007 ⁸ has shown that electron-affinic compounds which react with DNA free radicals have the potential to be universally active in combating hypoxia related radiosensitizers, and hypoxia specific cytotoxins such as tirapazamine (TPZ) is particularly active. Drugs can be selectively delivered to hypoxic tumours using either reductive enzymes or radiation produced free radicals to activate drug release from electron-affinic prodrugs such as TPZ. TPZ potentiates cell killing with fractionated irradiation. A linear relationship is known to exist between the sensitizer concentration required to produce a constant sensitizing response (C), and the one electron reduction potential at pH 7 (E^7): $-\log C = b_0 + b_1 E^7$. The relationship also holds for toxicity as well as sensitization. ⁹ [von Sonntag 2006] Intracellular thiols (eg glutathione, cysteine, and protein thiols) are known to have radioprotective qualities and suppression of these species can enhance chemotherapeutic efficacy.

TPZ is enzymatically bioreduced to a cytotoxic benzotriazinyl free radical as well as producing HO• radicals at very low levels of oxygen. Essentially nearly all of the DNA damage caused by TPZ occurs from radical species formed *inside* the nucleus, and TPZ radicals formed outside the nuclei do not contribute to DNA damage. ¹⁰ [Evans 1998] These free radicals cause DNA strand breaks. ¹¹⁻¹³ [Junnotula 2009, Brown 2004, Yin 2012]. The DNA damaging mechanism of TPZ and its analogues has been shown to be consistent with the release of the HO• radicals from the enzymatically reduced TPZ• radical. The HO• radical is now thought to be the agent principally responsible for DNA damage. ¹⁴ [Shen 2014]

Under normal oxygen conditions the intermediate free radical is rapidly oxidized back to TPZ. In cell lines TPZ been shown to be up to 450 times more cytotoxic in hypoxic compared to well-oxygenated cells, producing both single strand and double strand breaks. It is also known that severely hypoxic tumours require up to three times the radiation dose to kill tumours cells compared to oxic cells. ¹⁵ [Rowinsky 1999]

Preclinical results showed a synergistic chemoradiation relationship between TPZ and CisPt against a number of tumours, which was also found in Phase II trials. ¹⁶ [Green 2016]

However in a phase III trial a combined TPZ/CisPt chemoradiotherapy of cervical cancer was not found to be superior to standard CisPt chemoradiotherapy in either progression free survival or overall survival, although statistically there were inadequate progression or death events for a definitive result. A satisfactory TPZ/CisPt chemoradiotherapy starting dose was identified.¹⁷ [DiSilvestro 2014]

Despite promising results from a phase II trial of combined chemoradiotherapy of head and neck cancers using TPZ combined with CisPt, the phase III trial found no difference in patients (with advanced head and neck cancer not selected for the presence of hypoxia) in overall survival compared to CisPt chemoradiation alone.¹⁸ [Rischin 2010] It is unknown why the phase III trials of DiSilvestro and Rischin failed to reproduce the promising in vitro results or phase II trials of TPZ/CisPt treatments. It is also unknown whether the observed synergy that was found in cell lines or the phase II trials is due to TPZ exerting its hypoxic effect or its sensitizing of CisPt. The radio-resistance of hypoxic cells is related to the high electron affinity of the oxygen molecule, which enables even small amounts of oxygen (ca 0.01%) to fix radiation induced DNA damage before the damaged DNA can be restored by naturally occurring radical scavengers (eg thiols) in the cells.⁷ [Pettersen 2014] In vitro, the tumour-specific potentiation of cisplatin cytotoxicity is thought to result from an interaction between TPZ and cisplatin at the cellular level that requires low oxygen levels less than 1%. A marked time dependent scheduling effect was observed, with an increased cell kill potentiation when TPZ preceded CisPt administration.¹⁹ [Kovacs 1999] It is possible that varying levels of oxygen in tumours (median levels in various tumours span 0.1-4%) has confounded the phase III trial results, and drug delivery influences the relative intracellular concentrations of TPZ and CisPt and consequently intracellular oxygen levels which are critical to cell kill.

TPZ appears to undergo significant metabolic conversion before reaching its cellular DNA target based on the large change in efficacy between in vitro conditions (50–300 fold) and the observed 3-5 fold found in preclinical in vivo studies.²⁰⁻²⁴ [Denny 2009, Hicks 2006, Pruijn 2005, 2008, Hay 2003] The activity of TPZ in tumours is known to be compromised by its inefficient penetration into the hypoxic tissue. Hypoxic cells are the most distant from the functional oxygen supplying vasculature, so efficient extravascular transport is required for optimal TPZ efficacy. Modelling of TPZ in the tumour microvascular region showed a lack of transport penetration into the region lowers the cell killing in the most hypoxic region of the tumour by seven logs of activity. It is also possible that the reductive metabolism of TPZ is fast enough to lower its penetration into hypoxic tissue, thereby lowering its efficacy.²¹ [Hicks 2006]

Using an in vitro multilayered cell culture (MCC) model, when tirapazamine is administered via intravenous infusion, a stable TPZ distribution occurs within 15 minutes with cells most peripheral to the blood vessel were exposed to *only 10%* of the blood drug concentration. Extravascular penetration of TPZ to peripheral cells existing at low oxygen tension is limited by the metabolism of TPZ by more proximal cells existing at moderate oxygen tension, so TPZ is only significantly cytotoxic to cells located within ~75 µm of blood vessels,²⁵ [Kyle 1999] although other modelling suggests that hypoxic cells may be present within 25-50 µm of blood vessels.²⁶ [Ljungkvist 2002] Studies in mouse plasma and tumours have shown that peak plasma concentrations of TPZ were 26%, with the two electron reduction product, TPZ 1-oxide, being ca 15%, and the four electron reduction product, TPA nor-oxide, being ca. 1.5%. The KHT tumour:plasma ratio for TPZ was 32%, but for EMT6 tumours the ratio was only 7%. Extensive bioreduction metabolism occurred in tumour and normal tissue.²⁷

[Walton 1993] These studies clearly point to TPZ delivery to the intended target, hypoxic tumour cells, is the limiting factor affecting drug efficacy, particularly in the blood supply.

It has been suggested that the tumour microenvironment may be involved in the resistance of some solid tumour to chemotherapy, and that many anti-cancer drugs do not distribute efficiently and equally in body tissues. Poor and disorganized vascular networks, the absence of functional lymphatics that cause increased interstitial fluid pressure, and the composition and the structure of the extracellular matrix can slow down the transport of anti-cancer drugs within solid tumours. Hypoxia is a widely recognized hallmark of cancer in solid tumours. The microenvironment of solid tumours is known to be more acidic (pH 6.5–6.9) than the physiological pH of normal tissue (pH 7.2–7.5). Acidic microenvironments have been shown to increase the invasiveness of a tumor, leading to increased metastasis^{4,5} [Tredan 2007, Minchinton 2006]. It has also been found that a low pH can substantially potentiate the cytotoxic effect of TPZ in aerobic HT-29 human tumour cells, but no such potentiation was observed under hypoxic conditions.²⁸ [Skarsgard 1993] Using a magnetic resonance imaging/PISTOL technique to directly measure oxygen levels in pre-clinical tumour models of NSCLC (H1975) and epidermoid carcinoma (A431) treated with TPZ, it was found that tumour growth was not directly related to oxygen levels, but other factors such as tumour permeation and TPZ bio-reduction were probably involved as well as oxygen levels.²⁹ [Agarwal 2015]

The penetration of anti-cancer drugs into tumours is clearly a limiting factor in chemotherapeutic efficacy.^{2,4-6} [Tredan 2007, Minchinton 2006, Vaupel 2010, Muz 2015] There are other factors related to the vascular blood supply that limit the delivery of anti-cancer drugs to the targeted tumour sites. Recently there has been much interest in using cucurbit[n]urils (CB) as molecular delivery containers that enhance drug delivery to the intended target by protecting the drug from attack and degradation by biological agents.³⁰⁻³² [Saleh 2013, Nau 2011, Walker 2011] Many drugs have been found to be encapsulated within the cavity of CB, particularly cucurbit[7]urils, CB[7], and it may be that TPZ or some of its analogues may also form inclusion complexes with CB[7]. If this were so, then the formation of TPZ@CB[7] inclusion complexes may be beneficial in delivering increased quantities of TPZ compared to free TPZ to tumours and so increasing anti-cancer efficacy within the tumour.

We have previously developed a four parameter model that has been shown to apply to the transport and anti-cancer and metabolic efficacy of various drugs. The model, equation 1, is based on establishing linear free energy relationships between the four drug properties and various biological processes. Equation 1 has been previously applied to passive and facilitated diffusion of a wide range of drugs crossing the blood brain barrier, the active competitive transport of tyrosine kinase inhibitors by the hOCT3, OATP1A2 and OCT1 transporters, and cyclin-dependent kinase inhibitors and HIV-1 protease inhibitors. The model also applies to PARP inhibitors, the anti-bacterial and anti-malarial properties of fluoroquinolones, and active organic anion transporter drug membrane transport, and some competitive statin-CYP enzyme binding processes. There is strong independent evidence from the literature that $\Delta G_{\text{desolvation}}$, $\Delta G_{\text{lipophilicity}}$, the dipole moment and molecular volume are good inherent indicators of the transport or binding ability of drugs.³³⁻⁴⁰ [Fong 2015-16].

Equation 1:

$$\text{Transport or Binding} = \Delta G_{\text{desolvation}} + \Delta G_{\text{lipophilicity}} + \text{Dipole Moment} + \text{Molecular Volume}$$

Or

$$\text{Transport or Binding} = \Delta G_{\text{desolv,CDS}} + \Delta G_{\text{lipo,CDS}} + \text{Dipole Moment} + \text{Molecular Volume}$$

A modified form of equation 1 using the free energy of water desolvation ($\Delta G_{\text{desolv,CDS}}$) and the lipophilicity free energy ($\Delta G_{\text{lipo,CDS}}$) where CDS represents the non-electrostatic first solvation shell solvent properties, may be a better approximation of the cybotactic environment around the drug approaching or within the protein receptor pocket, or the cell membrane surface or the surface of a drug transporter, than the bulk water environment outside the receptor pocket or cell membrane surface. The CDS includes dispersion, cavitation, and covalent components of hydrogen bonding, hydrophobic effects. Desolvation of water from the drug ($\Delta G_{\text{desolv,CDS}}$) before binding in the receptor pocket is required, and hydrophobic interactions between the drug and protein ($\Delta G_{\text{lipo,CDS}}$) is a positive contribution to binding. $\Delta G_{\text{lipo,CDS}}$ is calculated from the solvation energy in n-octane. In some biological processes, where oxidation or reduction may be occurring, and the influence of molecular volume is small, the ionization potential or reduction potential has been included in place of the molecular volume. In other processes, the influence of some of the independent variables is small and can be eliminated to focus on the major determinants of biological activity.

The object of this study is to develop a quantum mechanical model based on identifying linear free energy relationships based on equation 1 which supplement the extensive multicellular layer pharmacokinetic/pharmacodynamic or structure activity modelling studies of Hicks, Pruijn and Hay²¹⁻²⁴ but may be more amenable to drug design by using in silico methods to examine molecular changes and their effects on biological activities. A secondary object is to see if TPZ can form inclusion complexes with CB[7] as a precursor to proof of principle of enhanced TPZ delivery to tumours which might be warrant further investigation.

2. Materials and Methods

All calculations were carried out using the Gaussian 09 package. Energy optimisations were at the DFT/B3LYP/6-31G(d,p) (6d, 7f) level of theory for all atoms. Selected optimisations at the DFT/B3LYP/6-311⁺G(d,p) (6d, 7f) level of theory gave very similar results to those at the lower level. Optimized structures were checked to ensure energy minima were located, with no negative frequencies. Energy calculations were conducted at the DFT/B3LYP/6-311+G(d,p) (6d, 7f) level of theory with optimised geometries in water, using the IEFPCM/SMD solvent model. With the 6-31G* basis set, the SMD model achieves mean unsigned errors of 0.6 - 1.0 kcal/mol in the solvation free energies of tested neutrals and mean unsigned errors of 4 kcal/mol on average for ions.⁴¹ [Marenich 2009] The 6-31G** basis set has been used to calculate absolute free energies of solvation and compare these data with experimental results for more than 500 neutral and charged compounds. The calculated values were in good agreement with experimental results across a wide range of compounds.^{42,43} [Rayne 2010, Rizzo 2006] Adding diffuse functions to the 6-31G* basis set (ie 6-31⁺G**) had no significant effect on the solvation energies with a difference of less than 1% observed in solvents, which is within the literature error range for the IEFPCM/SMD

solvent model. HOMO and LUMO calculations included both delocalized and localized orbitals (NBO).

Adiabatic electron affinities (AEA) in eV in water were calculated by the SCF difference between the optimised neutral and optimised radical species method as previously described. [Fong 2016] It has been shown that the B3LYP functional gives accurate electron affinities when tested against a large range of molecules, atoms, ions and radicals with an absolute maximum error of 0.2 eV.⁴⁴⁻⁴⁶ [Rienstra-Kiracofe 2002, Peverati 2014, Riley 2007]

It is noted that high computational accuracy for each species in different environments is not the focus of this study, but comparative differences between various species is the aim of the study. The literature values for D_s , D_{MCL} , HCR, IC_{50} to develop the multiple regression LFER equations have much higher experimental uncertainties than the calculated molecular properties. The statistical analyses include the multiple correlation coefficient R^2 , the F test of significance, standard errors for the estimates (SEE) and each of the variables $SE(\Delta G_{desolCDS})$, $SE(\Delta G_{lipoCDS})$, $SE(\text{Dipole Moment})$, $SE(\text{Molecular Volume})$, $SE(\text{AEA})$ as calculated from “t” distribution statistics. Residual analysis was used to identify outliers.

For the TPZ inclusion complex with cucurbit[7]uril (TPZ@CB[7]), energy optimisations were done at the DFT/B3LYP/3-21G level of theory, and using a two layer ONIOM model, at the 6-31+G(d,p) levels for the high level TPZ moiety, and using the UFF force field or semi-empirical PM6 at the low level. Energy calculations were done at the DFT/B3LYP/6-311+G(d,p) level of theory. The wB97XD functional was used for the TPZ@CB[7] thermodynamic calculations. This functional is a long range corrected hybrid with damped dispersion correction which gives good results with non-covalent and covalent systems and have been shown to give quite accurate results when compared to experimental data. The free energy of formation of the {TPZ@CB[7]} complex $\Delta G_{\text{form,Complex,sol}}$ in a particular solvent is calculated from the thermodynamic cycle at standard conditions, $T = 298.15 \text{ K}$ and $P = 1 \text{ atm}$:

$$\Delta G_{\text{form,Complex,sol}} = \Delta G_{\text{form,Gas}} + \Delta G_{\text{solv,Complex}} - \Delta G_{\text{solv,CB[7]}} - \Delta G_{\text{solv,TPZ}}$$

where $\Delta G_{\text{form,Gas}}$ is the free energy of formation of the complex in the gas phase, and ΔG_{solv} is the free energy of solvation. The $\Delta G_{\text{form,Complex}}$ are corrected for the BSSE (basis set supposition error) using the counterpoise method.

The binding of TPZ analogues 10 and 12 (shown in Figure 2(c)) to DNA using the structures shown in Figure 3(a), the full model, and 3(b), the truncated model of the {DNA-TPZ analogues}, for the neutral and protonated acridine species, as well as the diprotonated analogue 12 were investigated using the modified x-ray structure from PDB 366D⁵⁸ at the DFT/B3LYP/3-21G(d) level of theory for thermochemical analysis of the truncated model and the full model for energy. Energy calculations for the full model were also run using an Oniom model at the DFT/B3LYP/6-31+G(d) for the higher level and UFF for the lower level. Energy calculations for the truncated model were at the DFT/B3LYP/6-311+G(d,p) level of theory. Thermochemical analysis of the truncated model were also conducted at the DFT/wB97XD/3-21G(d) level of theory to test for significant dispersion effects between the intercalated acridine moieties and the guanine nucleobases, whereas the DFT/B3LYP/3-21G(d) level may be more appropriate for testing for induction (from the permanent dipole of the charged acridine) mixed with dispersion.⁵⁹ The $\Delta H_{\text{form,complex,sol}}$ for the {DNA-TPZ10} and protonated acridine complex {DNA-TPZ(H⁺)} were -34.6 and -22.8 kcal/mol respectively at the DFT/B3LYP/3-21G(d) and -28.2 and -15.5 kcal/mol at the DFT/wB97XD/3-21G(d) level. It is unclear whether intercalation is driven by dispersion

effects or a mixture of dispersion and induction, but these results show that the comparative differences between the two functionals is much the same for the unprotonated and protonated {DNA-TPZ} complexes. Corrections for the basis set supposition error using the counterpoise method were made. Solvation energies were calculated using the SMD model. In all cases, the HOMO was located on the guanine nucleobases of the DNA moiety for the neutral intercalated acridine species, but for the protonated acridine species, the HOMO was located on the two guanine bases *and* the intercalated N- protonated acridine in water and in vacuo.

3. Results

Hicks 2006 has used three-dimensional tissue cultures to model the extravascular transport and the vivo activity of range of TPZ derivatives. Hicks found that extravascular transport in tumours can be predicted by measuring drug penetration through colon cancer multicellular layers (MCL). A strong correlation was found between tumour drug levels generated using the extravascular transport model and hypoxic cell kill. Hay has examined the structure activity relationships amongst a range of TPZ analogues.²⁴ [Hay 2003] Pruijn 2005²² has similarly shown that diffusion in MCL tumour tissue was sigmoidally dependent on lipophilicity (log P from octanol-water partitioning), inversely proportional to $M^{0.5}$ (where M is the molecular weight), and strongly influenced cell kill.²² [Prujn 2005] This study uses Hicks', Hay's and Pruijn's experimental data to examine the applicability of eq 1 to the transport and tumour cell kill of the TPZ derivatives. All these studies were conducted in the same laboratory, which gives internally consistent data and eliminates the very large inter-laboratory variability which introduces unknown data population statistical errors or biases found in many published QSAR or LFER studies of biological processes.³³ [Fong 2016]

The structure of TPZ is shown in Figure 1 and the properties of the various analogues with substituents at positions 5, 6, 7 and 8 are given in Table 1. Figures 2(a),(b), and (c) show the TPZ analogues examined by Hicks, Pruijn and Hay²¹⁻²⁴ with a diverse range of 3-NH(R) substituents, with properties given in Table 1. All molecular properties in Table 1 were calculated using DFT/B3LYP/6-311⁺G(d,p) (6d, 7f) quantum mechanical methods as given in the experimental section.

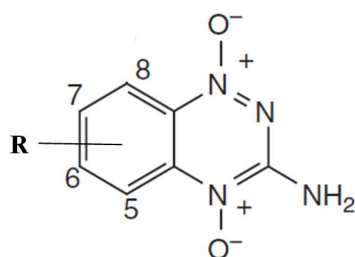


Figure 1. Tirapazamine (TPZ)

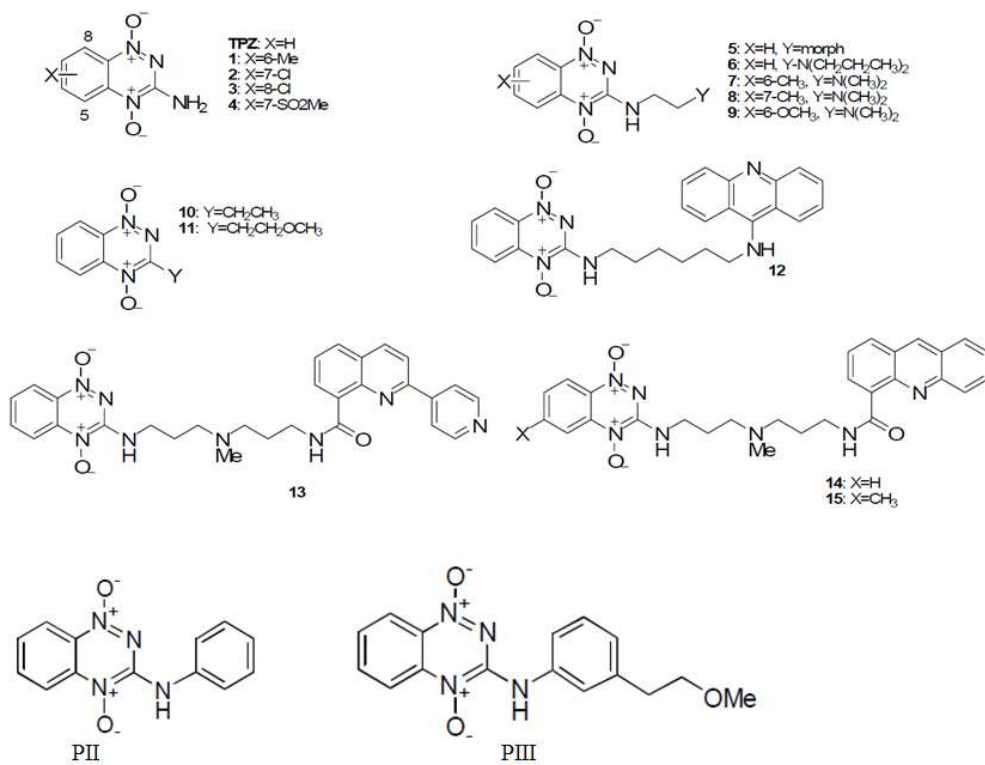


Figure 2a. TPZ analogues from Hicks 2006 Supplement Table 1

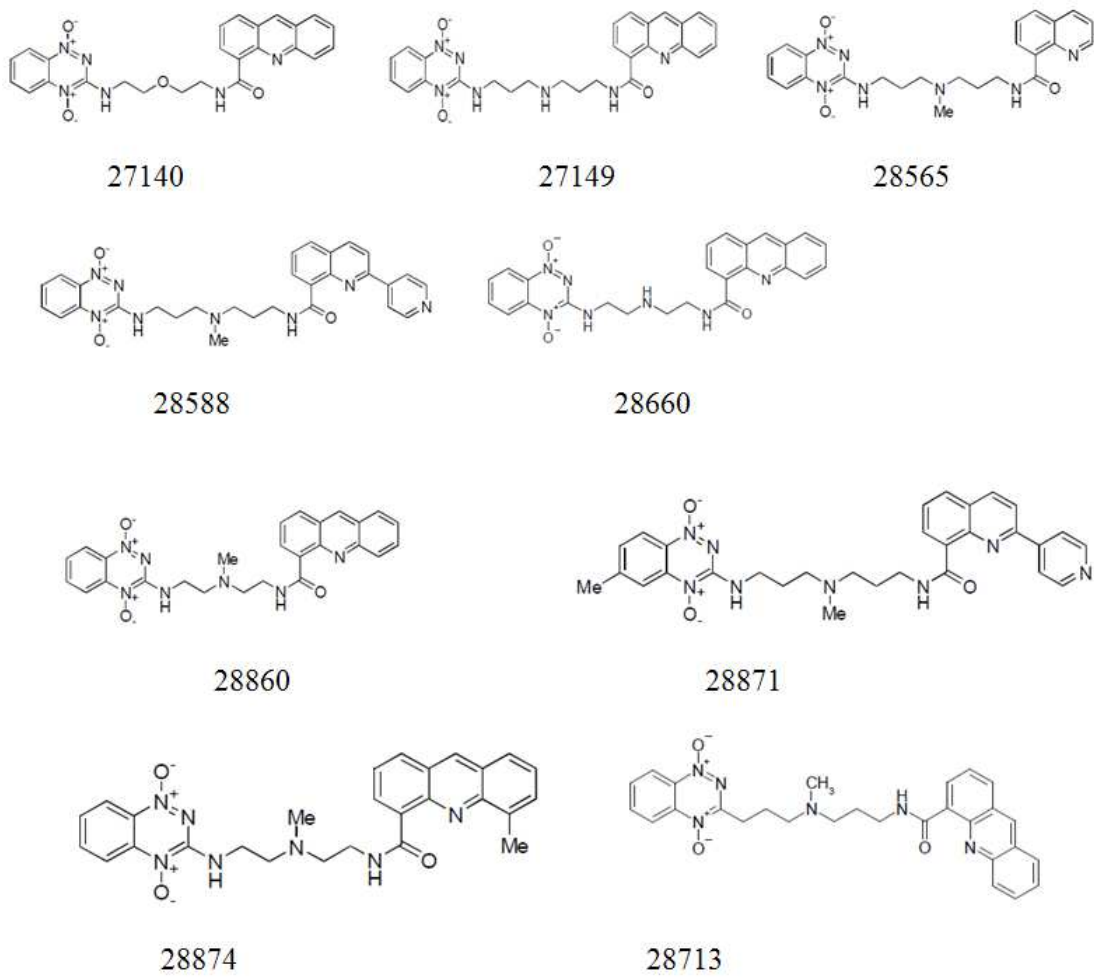


Figure 2b. TPZ analogues from Pruijn 2008 Supplement Table 1

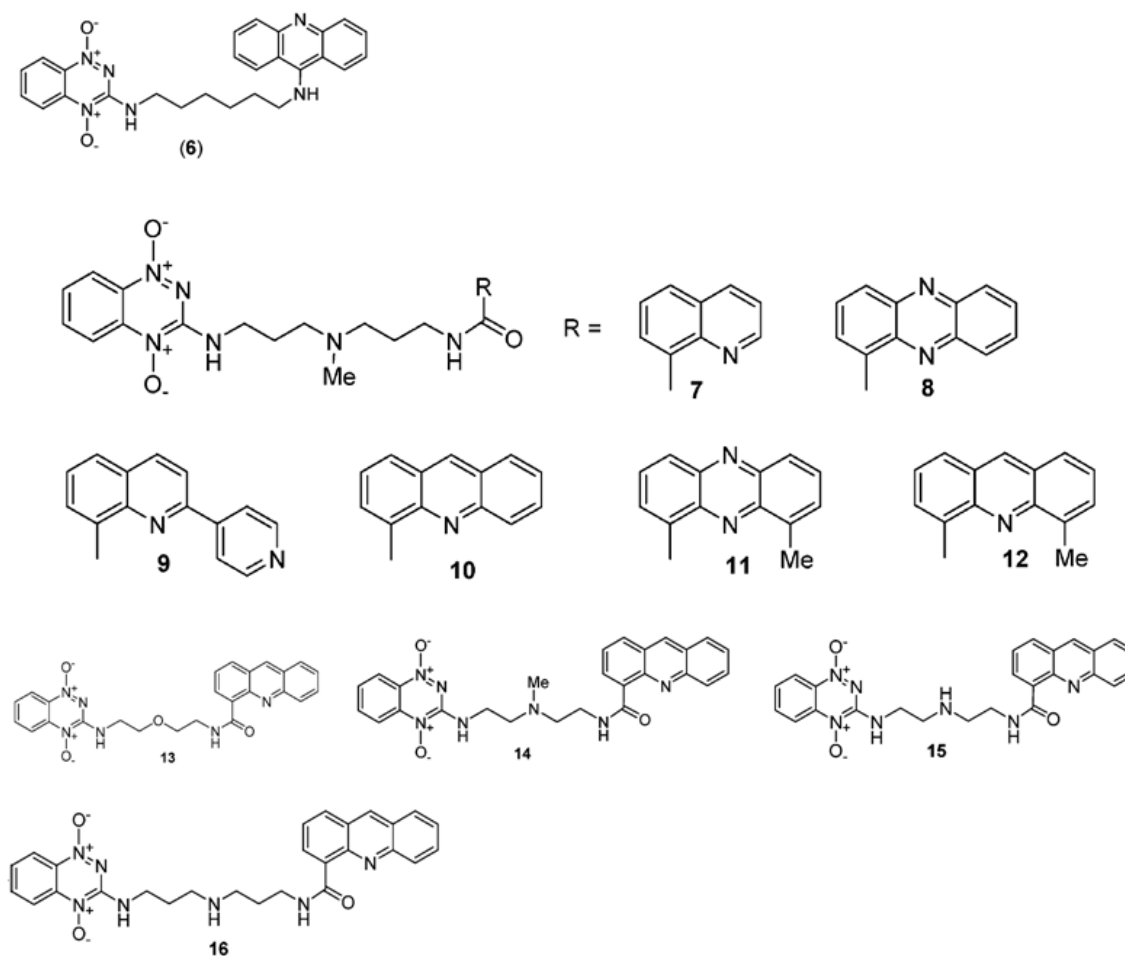


Figure 2c. TPZ analogues from Hay 2004 Table 1: DNA binding constants

3.1 Diffusion

Diffusion of 14 TPZ derivatives and 3 reference compounds through the collagen coated artificial Teflon support membranes D_s from Pruijn 2005 Table 1 (acridone, mannitol, urea, TPZ, 6-Me, 7-Me, 8-Me, 7-SO₂Me, 8-SO₂Me, 6-Cl, 7-Cl, 8-Cl, 7-CF₃, 8-CF₃, 8-NET₂, PII, PIII)

Eq 2

$$D_s = -0.040\Delta G_{\text{desolv,CDS}} + 0.025\Delta G_{\text{lipo,CDS}} + 0.034\text{Dipole Moment} - 0.07\text{Molecular Volume} + 1.90$$

Where $R^2 = 0.846$, $SEE = 0.122$, $SE(\Delta G_{\text{desolvCDS}}) = 0.040$, $SE(\Delta G_{\text{lipoCDS}}) = 0.026$, $SE(\text{Dipole Moment}) = 0.018$, $SE(\text{Molecular Volume}) = 0.002$, $F=16.47$, $\text{Significance}=0.0000$

Diffusion of 14 TPZ derivatives and 1 reference compound through the artificial Teflon support membranes coated with HT29 MCL, D_{MCL} from Pruijn 2005 Table 1 (excluding acridone and urea as outliers)

Eq 2a

$$D_{\text{MCL}} = -0.267\Delta G_{\text{desolv,CDS}} - 0.225\Delta G_{\text{lipo,CDS}} - 0.156\text{Dipole Moment} + 0.02\text{Molecular Volume} - 1.99$$

Where $R^2 = 0.858$, $SEE = 0.333$, $SE(\Delta G_{\text{desolvCDS}}) = 0.141$, $SE(\Delta G_{\text{lipoCDS}}) = 0.073$, $SE(\text{Dipole Moment}) = 0.060$, $SE(\text{Molecular Volume}) = 0.005$, $F=15.08$, $\text{Significance}=0.0003$

Diffusion of 32 TPZ derivatives through the artificial Teflon support membranes coated with HT29 MCL, D_{MCL} from Pruijn 2005 Table 1, Pruijn 2008 Table S1, and Hicks 2006 Supplemental Table 1 (excluding acridone and #13 as outliers) see Figures 2a and 2b.

Eq 3

$$D_{MCL} = -0.280\Delta G_{desolv,CDS} - 0.080\Delta G_{lipo,CDS} - 0.128\text{Dipole Moment} - 0.014\text{Molecular Volume} - 0.585$$

Where $R^2 = 0.474$, $SEE = 0.530$, $SE(\Delta G_{desolvCDS}) = 0.084$, $SE(\Delta G_{lipoCDS}) = 0.077$, $SE(\text{Dipole Moment}) = 0.051$, $SE(\text{Molecular Volume}) = 0.031$, $F=5.57$, $\text{Significance}=0.0024$

Diffusion of 14 TPZ derivatives and 3 reference compounds *as radical anions* through the collagen coated artificial Teflon support membranes D_s from Pruijn 2005 Table 1

Eq 4

$$D_s = -0.077\Delta G_{desolv,CDS} + 0.056\Delta G_{lipo,CDS} - 0.007\text{Dipole Moment} - 0.02\text{Molecular Volume} + 2.035$$

Where $R^2 = 0.870$, $SEE = 0.112$, $SE(\Delta G_{desolvCDS}) = 0.053$, $SE(\Delta G_{lipoCDS}) = 0.020$, $SE(\text{Dipole Moment}) = 0.016$, $SE(\text{Molecular Volume}) = 0.002$, $F=20.02$, $\text{Significance}=0.000$

Diffusion of 14 TPZ derivatives and 1 reference compounds *as radical anions* through the artificial Teflon support membranes coated with HT29 MCL, D_{MCL} from Pruijn 2005 Table 1 (excluding acridone and urea as outliers)

Eq 5

$$D_{MCL} = -0.447\Delta G_{desolv,CDS} - 0.300\Delta G_{lipo,CDS} + 0.039\text{Dipole Moment} - 0.12\text{Molecular Volume} - 2.175$$

Where $R^2 = 0.823$, $SEE = 0.370$, $SE(\Delta G_{desolvCDS}) = 0.193$, $SE(\Delta G_{lipoCDS}) = 0.075$, $SE(\text{Dipole Moment}) = 0.061$, $SE(\text{Molecular Volume}) = 0.008$, $F=11.65$, $\text{Significance}=0.001$

NB: Eqs 2-5 use molecular volumes which are 0.1 times the raw values (which ca. >10 times larger than the other 3 variables) to place these values on a comparative normalized basis.

3.2 Antiproliferative assays IC_{50}

IC_{50} μM of 14 TPZ derivatives hypoxic HT29 cells Hicks Supplemental Table 1 (excluding compounds 2 and 6 as outliers)

Eq 6

$$IC_{50} = 0.04\Delta G_{desolv,CDS} + 1.07\Delta G_{lipo,CDS} + 0.74\text{Dipole Moment} + 4.855\text{AEA} - 7.74$$

Where $R^2 = 0.626$, $SEE = 2.42$, $SE(\Delta G_{desolvCDS}) = 0.76$, $SE(\Delta G_{lipoCDS}) = 0.41$, $SE(\text{Dipole Moment}) = 0.40$, $SE(\text{AEA}) = 12.43$, $F=3.77$, $\text{Significance}=0.045$

Or

Eq 6a

$$IC_{50} = 1.09\Delta G_{lipo,CDS} + 0.70\text{Dipole Moment} + 2.78\text{AEA} - 1.53$$

Where $R^2 = 0.619$, $SEE = 2.32$, $SE(\Delta G_{lipoCDS}) = 0.39$, $SE(\text{Dipole Moment}) = 0.37$, $SE(\text{AEA}) = 10.81$, $F=5.43$, $\text{Significance}=0.017$

IC_{50} μM of 14 TPZ derivatives hypoxic HT29 cells *as radical anions* Hicks Supplemental Table 1 (excluding compounds 2 and 6 as outliers)

Eq 7

$$IC_{50} = 0.10\Delta G_{desolv,CDS} + 0.51\Delta G_{lipo,CDS} + 0.03\text{Dipole Moment} + 15.63\text{AEA} - 48.51$$

Where $R^2 = 0.470$, $SEE = 2.88$, $SE(\Delta G_{desolvCDS}) = 0.96$, $SE(\Delta G_{lipoCDS}) = 1.42$, $SE(\text{Dipole Moment}) = 0.46$, $SE(\text{AEA}) = 13.40$, $F=1.99$, $\text{Significance}=0.18$

or

Eq 7a

$$IC_{50} = 0.42\Delta G_{lipo,CDS} + 15.06\text{AEA} - 47.29$$

Where $R^2 = 0.468$, $SEE = 2.61$, $SE(\Delta G_{\text{lipoCDS}}) = 0.19$, $SE(\text{AEA}) = 9.75$, $F=4.84$, $\text{Significance}=0.031$

Eqs 6 and 7 were derived after showing that molecular volume had a very small influence on IC_{50} . $\Delta G_{\text{desolv,CDS}}$ can be eliminated from both eqs 6a and 7a, and dipole moment can be eliminated from eq 7a as well in view of their minor contributions.

3.3 Hypoxic cytotoxic ratio (HCR is the ratio of aerobic IC_{50} to anoxic IC_{50})

HCR of 15 TPZ derivatives hypoxic HT29 cells Hicks Supplemental Table 1 (excluding compound 7 as outlier)

Eq 8

$$\text{HCR} = -3.68\Delta G_{\text{lipo,CDS}} + 4.21\text{Dipole Moment} - 88.43\text{AEA} + 318.60$$

Where $R^2 = 0.510$, $SEE = 34.18$, $SE(\Delta G_{\text{lipoCDS}}) = 5.24$, $SE(\text{Dipole Moment}) = 5.04$, $SE(\text{AEA}) = 143.26$, $F=3.83$, $\text{Significance}=0.042$

HCR of 15 TPZ derivatives *as radical anions*, hypoxic HT29 cells, Hicks Supplemental Table 1 (excluding compound 7 as outlier)

Eq 9

$$\text{HCR} = -51.38\Delta G_{\text{lipo,CDS}} - 14.50\text{Dipole Moment} - 62.43\text{AEA} + 36.06$$

Where $R^2 = 0.664$, $SEE = 32.58$, $SE(\Delta G_{\text{lipoCDS}}) = 13.98$, $SE(\text{Dipole Moment}) = 4.46$, $SE(\text{AEA}) = 119.51$, $F=7.24$, $\text{Significance}=0.006$

Eqs 8 and 9 showed very small dependencies on $\Delta G_{\text{desolv,CDS}}$ and molecular volume, so these variables were eliminated.

Clonogenic assay data for 30 TPZ analogues as radical anions in SCCVII cells, $C_{10(\text{hyp})}$ μM from Hay 2003 Table 2

Eq 10

$$C_{10(\text{hyp})} = -43.60\Delta G_{\text{desolv,CDS}} + 46.29\Delta G_{\text{lipo,CDS}} + 36.36\text{Dipole Moment} + 50.47\text{AEA} + 157.53$$

Where $R^2 = 0.741$, $SEE = 50.20$, $SE(\Delta G_{\text{desolvCDS}}) = 15.70$, $SE(\Delta G_{\text{lipoCDS}}) = 18.13$, $SE(\text{Dipole Moment}) = 5.52$, $SE(\text{AEA}) = 76.94$, $F=17.92$, $\text{Significance}=0.000$

Clonogenic assay data for 29 TPZ analogues as radical anions in SCCVII cells, $C_{10(\text{aer})}$ μM from Hay 2003 Table 2

Eq 11a

$$C_{10(\text{aer})} = 116.10\Delta G_{\text{desolv,CDS}} - 246.84\Delta G_{\text{lipo,CDS}} - 3.90\text{Dipole Moment} - 2244.95\text{AEA} + 8065.46$$

Where $R^2 = 0.193$, $SEE = 1045.38$, $SE(\Delta G_{\text{desolvCDS}}) = 327.57$, $SE(\Delta G_{\text{lipoCDS}}) = 387.07$, $SE(\text{Dipole Moment}) = 118.69$, $SE(\text{AEA}) = 1602.48$, $F=1.44$, $\text{Significance}=0.251$

or

Eq 11b

$$C_{10(\text{aer})} = -2453.29\text{AEA} + 8628.36$$

Where $R^2 = 0.156$, $SEE = 1008.30$, $SE(\text{AEA}) = 1098.83$, $F=5.00$, $\text{Significance}=0.034$

Eq 11a and 11b (eliminating the non-significant dependencies on $\Delta G_{\text{desolv,CDS}}$, $\Delta G_{\text{lipo,CDS}}$ and dipole moment) for the aerobic assays are far poorer correlations than eq 10 for the hypoxic assay which may reflect some experimental discrepancies, and the HCR correlation is accordingly poor since HCR is the ratio of $C_{10(\text{aer})}$: $C_{10(\text{hyp})}$. Despite the low precision of the aerobic correlations, the reversal of dependency on the AEA is noteworthy and consistent with dominant free radical behaviour.

3.4 Linear relationship between adiabatic electron affinity in water (AEA in eV) and the experimental E(1) in V determined by pulse radiolysis from Hay 2003, Table 1, for 30 TPZ analogues.

Eq 12a

$$\text{AEA} = -1.451 \text{ E}(1) + 4.208$$

Where $R^2 = 0.672$, $\text{SEE} = 0.100$, $\text{SEE}(1) = 0.000$, $\text{SEIntercept} = 0.084$, $F=57.24$, $\text{Significance}=0.00000$

or eliminating 4 large outliers (7Cl, 7CF₃, 7NO₂, 6CF₃ analogues)

Eq 12b

$$\text{AEA} = -1.512 \text{ E}(1) + 4.250$$

Where $R^2 = 0.925$, $\text{SEE} = 0.041$, $\text{SEE}(1) = 0.000$, $\text{SEIntercept} = 0.040$, $F=295.04$, $\text{Significance}=0.00000$

3.5 Linear relationship between $\Delta G_{\text{lipo,CDS}}$ and log P (experimental n-octanol/water partition coefficient) for 33 TPZ analogues taken from Hay 2003, Pruijn 2005, and Hicks 2006.

Eq 13a

$$\Delta G_{\text{lipo,CDS}} = -1.794 \log P - 7.400$$

Where $R^2 = 0.357$, $\text{SEE} = 2.784$, $\text{SElogP} = 0.432$, $F=17.21$, $\text{Significance}=0.00024$

or

Eq 13b

$$\Delta G_{\text{lipo,CDS}} = -1.083 \log P - 7.093$$

Where $R^2 = 0.389$, $\text{SEE} = 1.255$, $\text{SElogP} = 0.283$, $F=14.62$, $\text{Significance}=0.00087$

Eq 13a includes several large outliers particularly compounds 12-15 from Hicks 2006 supplemental table 1, as shown in Figure 2, which are 3-NH-R compounds where R are large side chains with polycyclic aromatic groups, acridone, and the 6CF₃, 7CF₃ and 8CF₃ substituted TPZ analogues. However the linear relationship is highly significant, and there are known problems with some log P partitioning data. Eq 13b shows the correlation excluding the 8 outliers, where the SEE and SElogP are significantly lower than in eq 13a.

3.6 DNA binding affinity of TPZ analogues

Hay^{24b} [Hay 2004] has shown that improved hypoxic tumour efficacy can be obtained by attaching DNA targeting substituents to TPZ, with the intention that substituents such as the DNA intercalating acridine moieties (chromophores) will bring the active TPZ moiety close to the target DNA such that improved cytotoxicity will result. The binding constants $K_{\text{DNA}} 10^4 \text{ M}^{-1}$ are taken from Hay 2004 Table 1 and the analogues are shown in Figure 2c. Hay has shown that binding affinity was dependent on the presence of a positive charge on the chromophore or the linking side chain as adjudged by calculated pKa values. In this study the neutral species, mono-protonated species (protonated at the side chain amine group *or* the chromophore group) and the di-protonated species (protonated at the side chain amine group *and* the chromophore group) were examined and tested against equation 1 to see if any indication could be discovered about where the TPZ analogues might be protonated when binding to DNA. Correlations against the neutral species, the mono-protonated side chain species and di-protonated species were very poor. The best correlation was against the mono-protonated chromophores but only when compound 12 was considered as a di-protonated species (protonated at the acridine N and side chain N, and also when compound 13 was considered as the neutral species, otherwise these two compounds were large outliers from the correlation equation).

Eq 14

$$K_{\text{DNA}} = -14.51\Delta G_{\text{desolv,CDS}} + 5.60\Delta G_{\text{lipo,CDS}} + 0.034\text{Dipole Moment} + 0.31\text{Molecular Volume} - 48.93$$

Where $R^2 = 0.920$, $\text{SEE} = 6.00$, $\text{SE}(\Delta G_{\text{desolv,CDS}}) = 2.48$, $\text{SE}(\Delta G_{\text{lipo,CDS}}) = 4.44$, $\text{SE}(\text{Dipole Moment}) = 0.43$, $\text{SE}(\text{Molecular Volume}) = 0.20$, $F=17.31$, $\text{Significance}=0.002$

Eq 14a shows the correlation in eq 14 but with the compound 13 as the protonated species where the correlation is significantly poorer, but shows the same characteristics with the DNA binding being dominantly driven by desolvation and lipophilicity.

Eq 14a

$$K_{\text{DNA}} = -9.49\Delta G_{\text{desolv,CDS}} - 2.90\Delta G_{\text{lipo,CDS}} + 0.18\text{Dipole Moment} + 0.19\text{Molecular Volume} - 120.76$$

Where $R^2 = 0.749$, $\text{SEE} = 10.65$, $\text{SE}(\Delta G_{\text{desolv,CDS}}) = 4.39$, $\text{SE}(\Delta G_{\text{lipo,CDS}}) = 7.30$, $\text{SE}(\text{Dipole Moment}) = 1.27$, $\text{SE}(\text{Molecular Volume}) = 0.43$, $F=4.47$, $\text{Significance}=0.051$

Hays' binding study ^{24b} [Hay 2004] contains no direct evidence about how the potentially DNA intercalating acridine moieties can bring the active TPZ moiety close to the target DNA so that improved cytotoxicity will result. Molecular models of the interaction of TPZ analogues 10 and 12 (see Figure 2(c)) have been produced based on the x-ray structure of N-(2-(dimethylamino)ethyl)acridine-4-carboxamide (DACA) into DNA: X-ray structure complexed to d(CG(5-BrU)ACG)2 at 1.3 Å resolution. ⁵⁸ [Todd 1999] The structure of {DNA-TPZ analogue12} complex is shown in Figure 3(a) along with a truncated model Figure 3(b) used to derive comparative binding constants between analogues 10 and 12 (protonated and un-protonated forms in water) and the DNA moiety.

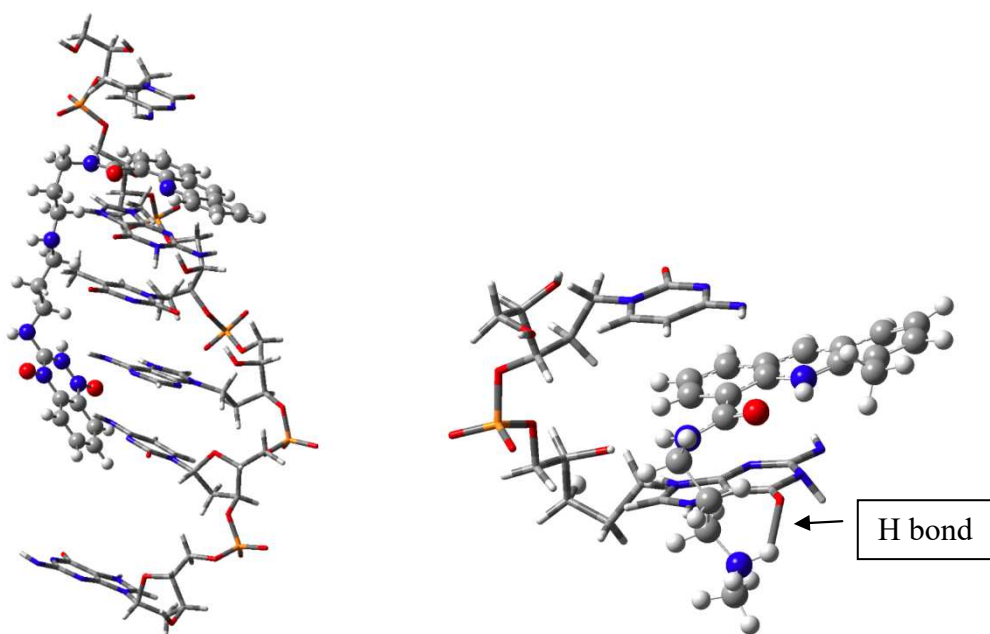


Figure 3 (a) {DNA-TPZ analogue 10} complex showing acridine moiety intercalated between two guanine nucleobases of DNA moiety and Figure 3(b) showing the truncated model of Figure 3 (a) showing the TPZ analogue 12 with acridine moiety protonated at N and methyl group at position 9, and the aminopropyl side chain protonated at N and hydrogen bonded to the O of the nearby guanine nucleobase of the DNA moiety.

Since eq 14 and 14(a) indicate that the binding of TPZ analogues to DNA is predominantly driven by desolvation and lipophilicity effects, the truncated model of the {DNA-TPZ analogues} has been investigated for analogue 10 and 12, for the neutral and protonated acridine species, as well as the diprotonated analogue 12, since eq 14(a) suggests this form may be dominant in equilibrated solution.

A thermochemical binding model which is routinely used to calculate binding in solution (see experimental) has been used which involves calculating the binding in vacuo, then correcting for the solvation of the complex using the solvation of the ligand and DNA individually. Only the comparative differences amongst the complexes are meaningful, since the model structure represents only a small portion of the {DNA-TPZ analogue} complexes, but the model should be able to differentiate between DNA interaction with neutral and protonated species, particularly since solvation effects would be quite different for charged versus neutral analogues.

The free enthalpy of complex formation in solution, $\Delta H_{\text{form,complex,sol}}$ of the TPZ10 analogue and its acridine N-protonated form is -34.6 and -22.8 kcal/mol, where the configurational entropy, $T\Delta S_{\text{form,complex,sol}}$ at 298.15K were -17.3 and -18.6 kcal/mol. For the {DNA complex-TPZ12 analogue} model complex, $\Delta H_{\text{form,complex,sol}}$ for the TPZ analogue and its acridine N-protonated form were -35.7 and -31.0 kcal/mol, with $T\Delta S_{\text{form,complex,sol}}$ values of -17.2 and -18.6 kcal/mol. For both analogues, the complex bindings in vacuo were greater for the acridine N-protonated forms, consistent with the highest occupied molecular orbitals HOMO for the complex being delocalized over the two guanine nucleobases and the intercalated acridine N-protonated moiety. This delocalization does not occur for the neutral species where the acridine moiety carries no formal charge. Despite the greater binding in vacuo for the acridine N-protonated complexes, the greater desolvation energy required for the charged TPZ analogues and the DNA moiety override the binding efficacy producing weaker total overall binding efficacy for the charged species in water.

For the diprotonated TPZ12 analogue, the $\Delta H_{\text{form,complex,sol}}$ is -54.3 kcal/mol, with $T\Delta S_{\text{form,complex,sol}}$ of -15.2 kcal/mol, which compared with the monoprotated N-acridine complex of -31.0 and -18.6 kcal/mol respectively. This results shows that protonation of the side chain amino-propyl at N which allows hydrogen bonding to one of the guanine oxygen atoms (bond length 2.62 Å) substantially enhances complex binding (see hydrogen bond indicated in Figure 3(b)).

3.7 DFT modelling of TPZ@CB[7]

Figures 4(a) and (b) show an “internal configuration” of the TPZ@CB[7] complex in water, where the TPZ is inside the hydrophobic cavity region of CB[7]. Figure 4(c) shows the “external configuration” where the TPZ is attached to the polar carbonyl portal region of CB[7]. The free enthalpy of complex formation in solution, $\Delta H_{\text{form,complex,sol}}$ of the internal configuration is -12.8 kcal/mol compared to -4.0 for the external configuration. These values suggest that these complexes may be stable and capable of synthesis. It is noted that these values include large configurational entropy $T\Delta S$ and small $\Delta G_{\text{form,complex,sol}}$ values, and were corrected for the basis set supposition error. A thermodynamic cycle was used for the free energy calculations.

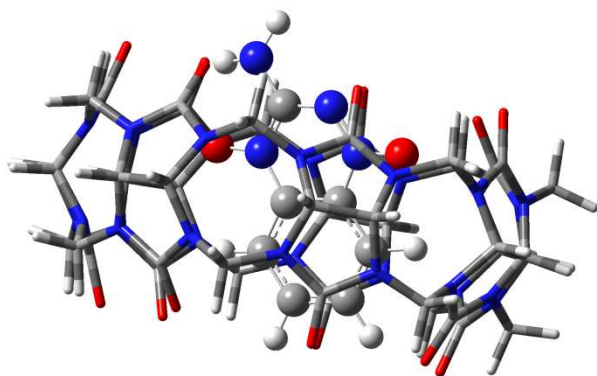


Figure 4(a) TPZ@CB[7] complex internal configuration side view

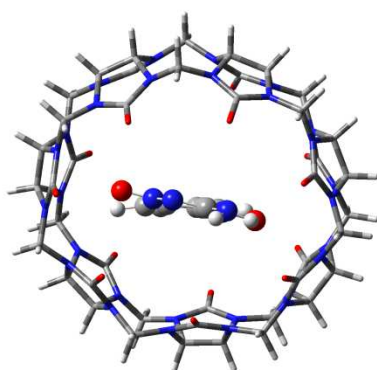


Figure 4(b) TPZ@CB[7] complex internal configuration top view

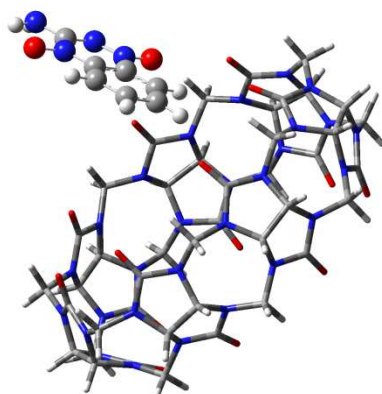


Figure 4(c) TPZ@CB[7] complex external configuration

Previous computational studies of the dynamics of guest insertion into the CB cavity have shown that high energy water in the cavity is expelled as the guest drug enters the hydrophobic cavity.^{31,40} [Nau 2011, Fong 2017] In this study the configurations of the TPZ@CB[7] were varied from the “external configuration” to the “internal configuration”

using the SMD solvent model. The SMD model calculates the solvation free energy as electrostatic component and the non-electrostatic component, $\Delta G_{\text{CDS,water}}$. The values of $\Delta G_{\text{CDS,water}}$ vary smoothly from -19.0 to 13.6 kcal/mol depending how deeply embedded the TPZ is in the CB[7] cavity; and the degree of openness of the carbonyl group portals in the CB[7]. The carbonyl portal opening can be closed or open when inserting guest molecules. Using the $\Delta G_{\text{CDS,water}}$ value as a measure of the free energy change as water molecules are expelled, a linear relationship has been found between the total energy of the solvated TPZ@CB[7] complex $\Delta E_{\text{total,water}}$ for ten separate configurations moving from the “external” to the “internal” configuration and $\Delta G_{\text{CDS,water}}$:

$$\Delta E_{\text{total,water}} = -26.6 \Delta G_{\text{CDS,water}} + 385.0 \text{ for } n=10, R^2 = 0.898, F = 80.54, \text{ significance} = 0.0000$$

This relationship gives an indication of the solvation energy changes involved in a TPZ molecule entering (and the reverse process leaving) the CB[7] cavity and may have relevance to how easily TPZ could be released from the TPZ@CB[7] complex.

4. Discussion

The accepted model of TPZ drug diffusion into the tumour (Figure 5) is (a) TPZ from the blood vessels surrounding the tumour enters the ECM and can permeate into the cells nearby the blood vessels where oxygen levels are high, so oxyc cells have sufficient oxygen to prevent metabolism of TPZ and cytotoxicity (b) the composition and structure of the ECM affects the rate of drug diffusion, the chemical and physical properties of the TPZ analogues affects the diffusion rate, and increased water solubility of drugs increases transport through the ECM compared to more lipophilic drugs which can permeate cell membranes more easily [5] [Minchinton 2006] (c) further diffusion of TPZ occurs through the ECM until it reaches the hypoxic regions of the tumour, where permeation into hypoxic cells can occur and metabolism can occur in the cytosol, and considerable binding of TPZ with proteins can also occur to reduce overall TPZ concentrations (d) TPZ can enter the nucleus where bioreduction occurs to produce the TPZ• and HO• radicals which cause DNA damage. The extent of damage depends on the concentrations of the TPZ• and HO• radicals and the oxygen tension. It is clear that there is a trade-off between the diffusion rate of a TPZ analogue (and the degree of metabolic consumption) and the rate of enzymatic reduction and consequent hypoxic cytotoxicity.

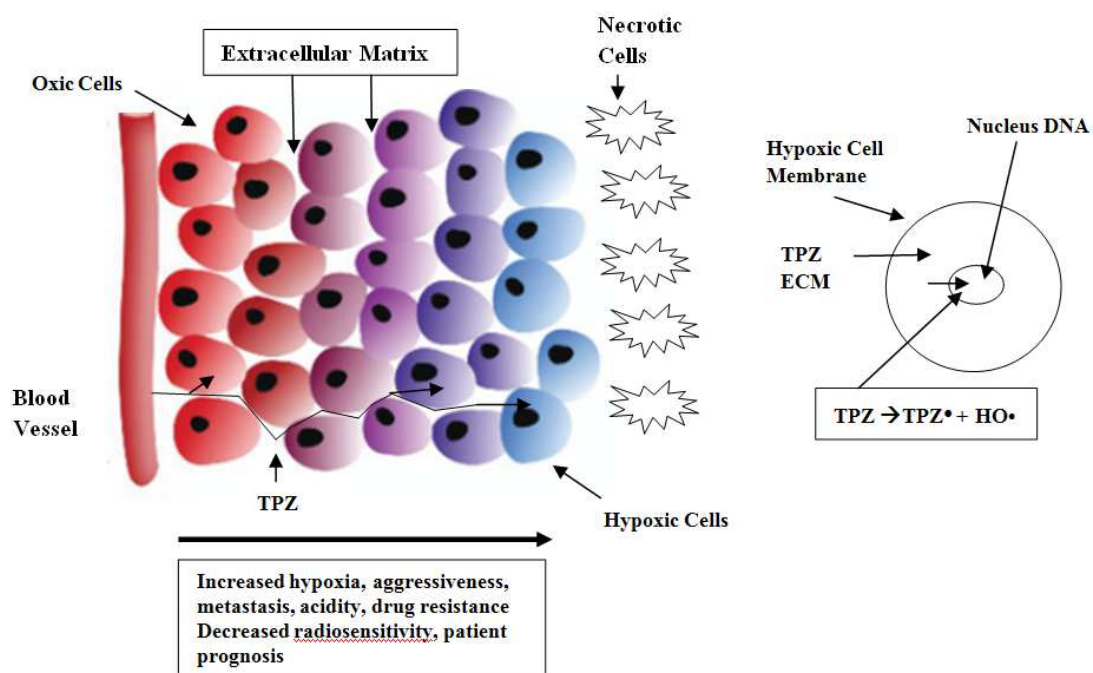


Figure 5. Schematic representation of extravascular transport of TPZ analogues and cytotoxicity of hypoxic tumour cell induced by bioreduction of TPZ to form radical species in cell nucleus.

Multicellular layers (MCL) have been shown to be representative of many of the properties of solid tumours, such as the generation of an ECM, gradients of nutrient concentration and cell proliferation, and regions of hypoxia and necrosis in thicker layers. MCL are effective models for the extravascular region of tumours. ^{5,21-24} [Minchinton 2006, Hicks 2006, Pruijn 2005,2008 and Hay 2003]

4.1 Diffusion of TPZ analogues

We have previously shown that the general form eq 1 applies to simple and facilitated diffusion of a range of drugs crossing the blood brain barrier. ³⁴ [Fong 2015] Eqs 2a and 2b can be directly compared to assess the difference in diffusion for the test set of TPZ derivatives between the collagen coated Teflon support membrane (which has a porosity of 11%, and pore size of 0.4 μm) and the MCL coated membrane. The D_{MCL} equation shows a negative increased dependency on the desolvation, lipophilicity and dipole moment compared to the D_{S} equation 2 but no change in dependency on molecular volume. Eq 2 represents Fickian diffusion behaviour as shown by Pruijn ^{22,23} so the some degree of desolvation occurs as the TPZ drugs pass through the support membrane and the MCL, and hydrophobic (or lipophilic) and polar (dipole moment) interactions are of almost equal importance in determining the diffusion rates, whilst the influence of molecular volume has positive dependency on diffusion.

Eq 3 shows a larger set of TPZanalogues than in eq 2a and 2b, notably the addition of a number of analogues which have large side chains as shown in Figures 2a and 2b which have been added to the analogues in Pruijn 2005 ²². Comparison of eq 2b with eq 3 shows that the

principal difference is the greater influence of lipophilicity, as shown by the larger $\Delta G_{\text{lipo,CDS}}$ value in eq 3. This outcome is in accord with the expected increased influence of the large lipophilic side chain analogues. However the influence of water desolvation, dipole moment and molecular volume is similar between eq 2b and eq 3. The influence of molecular volume is much larger than those exerted by lipophilicity, desolvation and dipole moment, suggesting that the primary mechanism of diffusion in this system is driven by desolvation of the TPZ analogues prior to entering the cellular membrane, followed by a polar or electrostatic interaction between the desolvated analogue and the outer hydrophilic head groups of the membrane phospholipid bilayer, followed by the ease that more lipophilic analogues can then permeate into the inner hydrophobic membrane bilayer, where molecular volume also has a large influence.³⁴ [Fong 2015]

Eq 3 can be compared with the equation derived by Pruijn 2008²³ where $\log D_{\text{MCL}} = a + b \log \text{MW} + c / 1 + \exp \{(\log P_{7.4} - x + y \cdot \text{HD} + z \cdot \text{HA})/w\}$ where MW is the molecular weight, $\log P_{7.4}$ is the octanol-water partition coefficient at pH 7.4, HD is the number of hydrogen bond donors, HA is the number of hydrogen bond acceptors, a is a constant, and b, c, x, y, z and w are statistically fitted coefficients. This equation is highly statistically significant, but does have 6 fitted coefficients. Eq 3 is similar to this equation in that lipophilicity and molecular volume are similar to $\log P_{7.4}$ and MW, dipole moment is similar to hydrogen bonding ability in that it represents dipolar interactions between the drug and the cell membrane, but there is no desolvation equivalent term in the Pruijn equation. We have previously shown that desolvation is a significant factor in cell membrane permeation and facilitated diffusion (as well as active transport processes).^{33,35,25,38} [Fong 2015, 2016]

Eq 4 and 5 show the diffusion behaviour if the TPZ species were anion radicals. This *hypothetical* situation (which assumes that diffusion of radical species is similar with that of neutral species but it is the charge on the radical anion which ultimately determines diffusion of these species) could exist under certain clinical situation where for example where ionizing radiation was being used, with TPZ acting as a radiosensitizer⁴⁷ [Seiwert 2006] such as might occur with when co-administered with cisplatin, or in hypoxic regions of a solid tumour, or where metabolic reduction had occurred. Pruijn 2005²² found that most of the investigated analogues were metabolically stable in HT29 MCLs, but six of the compounds with electron withdrawing substituents (7- and 8-SO₂Me, 5- and 8-Cl, 7- and 8-CF₃) were metabolized significantly. There is a 6 fold change in sensitivity for all 4 independent variables between eq 4 and 5, and Eq 3 can also be directly compared to eq 5, which is more relevant to possible clinical situations. Eq 5 shows a greater dependency on desolvation and positive dependency on dipole rather than a negative dependency for the neutral species. This observation is consistent with the increased charge spread over the TPZ moiety in the radical ions interacting with cellular electrochemical membrane potentials.³⁴ [Fong 2014] These data in eq 2-5 have implications for drug design since it is clear that transport of TPZ derivatives to its DNA target is dominated by desolvation, lipophilicity and dipole moment for the neutral species and may be even more so for radical species where desolvation and dipole are large factors. Molecular size is a minor contributor to the diffusion of the TPZ compounds.

Since it has been shown¹⁰ [Evans 1998] that enzymatic reduction of TPZ within the nucleus is the main mechanism of DNA damage (in human lung cancer cells), and that radical species formed outside the nucleus do not contribute to DNA damage, then the rate determining TPZ passive diffusion mechanism into the cell predominantly involves the neutral TPZ species, as portrayed by eq 3, and not the radical species, as portrayed by eq 5. It is well known that charged species do not easily permeate cell membranes compared to neutral species.³⁴ [Fong

2014] Passive diffusion appears to be the dominant transport mode, since TPZ is not a known substrate for active drug transporters, and HT29 cells do not express significant levels of P-gp or MRP-1 or -2^{22,48} [Pruijn 2005, Cummins 2002]

4.2 Antiproliferative assays IC₅₀

The IC₅₀ analyses eqs 7 and 7a for the radical TPZ analogues shows that anti-proliferation of hypoxic HT29 cells is dominated by the AEA, with a minor dependence on the lipophilicity. This results suggests that only electron transfer processes involving TPZ is important not any binding processes involving TPZ and DNA, since some larger dependences on desolvation, dipole and lipophilicity would be expected, similar to eq 6a, as has been found in other drug – membrane permeation interaction studies.^{34,38,39} [Fong 2015, 2016, 2016] TPZ is known to exerts its cytotoxic effects without forming adducts with macromolecules such as DNA.^{15,49,50} [Rowinsky 1999, Inbaraj 2003, Daniels 1998]

4.3 Hypoxic cytotoxic ratio

Eq 8 (as neutral species, but adding the AEA as separate extrinsic variable) and eq 9 (as radical anion species) for the HCR of 15 TPZ hypoxic derivatives in HT29 cells shows that the HCR is dominated by the dependency on the AEA as expected. However, eq 9 shows that the radical species show an equal dependence on the lipophilicity, $\Delta G_{\text{desolv,CDS}}$, as well as the AEA. It is also noted that the HOMO of the radical anions resides over the TPZ moiety for the 15 analogues studied, with the exception of compound 12 which has a 3-NH(R) structure where R contains a 9-substituted acridine moiety. In this case the HOMO resides on the acridine group, which potentially makes this side chain more reactive than the other side chains studied, and possibly induces a different mechanism where the acridine group interacts with DNA. The 15 TPZ derivatives have a wide range of structural differences but the TPZ moiety is the locus of activity.

The separate aerobic and hypoxic clonogenic assays for 30 TPZ analogues as radical anions in SCCVII cells are examined in eqs 10 and 11a, 11b. Eq 10 for the hypoxic assay shows a strong correlation with $C_{10(\text{hyp})}$ with desolvation, lipophilicity, dipole and AEA. However the correlation with $C_{10(\text{aer})}$ is far weaker which results in a poor correlation with HCR (not shown) since HCR is the ratio of $C_{10(\text{aer})} : C_{10(\text{hyp})}$. Given the strong correlation with HCR in eq 9, this result suggests some experimental discrepancies with the $C_{10(\text{aer})}$ data, which is surprising considering that the 30 TPZ analogues all have similar molecular structures with varying substituents, whereas the TPZ analogues tested in eq 9 have widely varying molecular structures. Eq 11b shows the correlation between $C_{10(\text{aer})}$ and AEA only. Despite the low precision of the aerobic correlations, the reversal of dependency on the AEA in eqs 10 and 11a or 11b is consistent with expected free radical behaviour where the aerobic behaviour is almost exclusively determined by the electron affinity of the TPZ analogues. Under aerobic conditions, it is thought that cellular toxicity is a result of reactive oxygen species, the superoxide radical which is much less toxic than the TPZ radical or hydroxyl radical, being formed by redox cycling of the TPZ radical with oxygen.⁵¹ [Brown 1999] So under aerobic conditions, the clonogenic assay is dominated by the AEA dependency, whereas under hypoxic conditions, desolvation, lipophilicity, the dipole moment and AEA are equal contributors to cytotoxicity, consistent with diffusion and or bioreduction processes being dominant. The $C_{10(\text{hyp})}$ results are consistent with the processes involving permeation of the TPZ analogues into the nucleus and bioreduction in the nucleus to form the TPZ and hydroxyl radicals, which interact with DNA as shown in Figure 5.

Since the TPZ analogues can permeate the cell membranes of oxic and hypoxic cells, but cytotoxicity mainly occurs in the nucleus of hypoxic cells and not by radicals formed in the cytosol¹⁰ [Evans 1998] then the $C_{10(\text{aer})}$ results are then consistent with free radical processes alone occurring in the ECM (strong dependency on AEA) and do not involve any membrane or enzymatic interaction processes (where dependencies on desolvation, lipophilicity and dipole moment would be expected in the correlations). The $C_{10(\text{aer})}$ results are also consistent with involvement by the superoxide radical which is much less toxic than the TPZ radical or hydroxyl radical, being formed by redox cycling of the TPZ radical with oxygen.⁵¹ [Brown 1999]

4.4 Linear relationship between adiabatic electron affinity in water (AEA in eV) and the experimental E(1) in V determined by pulse radiolysis

Eq 12a and 12b show a strong linear relationship between the AEA and experimental E(1). Removing the 4 largest outliers, the 7Cl, 7CF₃, 7NO₂, 6CF₃ analogues, which are all strong electron withdrawing substituents, gives a vastly improved correlation. The intercept of eq 12b gives a value of 4.28eV, which is in agreement with the SHE, which is the reference standard for the E(1) experimental values. The absolute potential of the aqueous standard hydrogen electrode is generally taken to be either 4.28V or 4.44V, which are derived from values of $\Delta G_s^*(\text{H}^+)$ of -1112.5 and -1098.9 kJ mol⁻¹ respectively. The value of 4.44 V includes an estimate of the contribution due to the surface potential of water. However since the total charge is conserved in a reaction, the contribution due to the surface potential cancels out in a chemically balanced chemical reaction that occurs in a single phase. The SMD model uses a $\Delta G_s^*(\text{H}^+)$ of -1112.5 kJ mol⁻¹ and SHE value of 4.28 V.^{41,52} [Ho 2016, Marenich 2009] This correlation gives confidence that DFT AEA calculations using the SMD water solvation model are good proxies for aqueous reduction potentials. Romalho 2004⁵³ has examined five 8-substituted TPZ analogues and found that B3LYP/6-311⁺⁺G(d,p) AEA calculations in water were in good agreement with experimental reduction potentials.

4.5 Linear relationship between $\Delta G_{\text{lipo,CDS}}$ and log P (experimental n-octanol/water partition coefficient) for 33 TPZ analogues

Eqs 13a and 13b show highly significant correlations between $\Delta G_{\text{lipo,CDS}}$ and log P, although there are a number of clear outliers: the 3-NH-R compounds where R are large side chains with polycyclic aromatic groups (compounds 12-15 in Figure 2), acridone, all of which are quite different molecules from the simple substituted TPZ derivatives, and the 6CF₃, 7CF₃ and 8CF₃ substituted TPZ analogues. Removing these outliers in eq 13b improves the correlation as adjudged by the lower standard errors (SE).

However there are several difficulties with log P values derived from n-octanol-water partitioning experiments. Wet octanol solution is a poor proxy for proteins or biological membranes because it contains ~2M of water, and cyclohexane would be a much better proxy. A set of solvation parameters derived for the protein interior from protein engineering data was also different from octanol scale: it was close to cyclohexane scale for nonpolar atoms but intermediate between cyclohexane and octanol scales for polar atoms.^{54,55} [Radicza 1988, Lomize 2012] We have previously used n-octane as a proxy for proteins or biological membranes as its dielectric properties closely resemble cyclohexane, and its long hydrocarbon chain is a better match to biological lipids. Experimental problems have been experienced with very hydrophilic or very hydrophobic compounds, usually because of

solubility issues, emulsion formation and the formation of micelles within the octanol phase, adsorption onto vessel walls). Other difficulties concerns compounds that can tautomerize or equilibrate between zwitterion and neutral form, and amphiphilic chemicals may behave as detergents.^{56,57} [Braumann, 1986; Dearden and Bresnen, 1988].

4.6 DNA binding affinity of TPZ analogues

Eqs 14 or 14a show that DNA binding is largely driven by ligand desolvation and lipophilicity for the protonated chromophores. The X-ray studies of DNA intercalated acridines complexes such as DACA, N-(2-(dimethylamino)ethyl)acridine-4-carboxamide have shown that (a) the side chain amine is protonated and hydrogen bonds to one of the two N7 sites of guanine at the intercalation site, (b) the acridine is protonated at N10 (c) both acid and conjugate base forms of acridine can be seen in the crystal structure (pH of crystallization 6.5), and (d) a third spacer drug was found between the two duplexes and is present as the monocationic (conjugate base form) with a neutral acridine ring.⁵⁸ [Todd 1999] Clearly the DNA intercalation of DACA and similar compounds is complex and multiple mechanisms and species are possible in solution leading to the crystallized complex forms. It is conceivable that eq14 which includes compound 13 as the neutral acridine species, and which does not have an amine side chain, may be valid. It is noted that eq 14 has treated compound 12 as the diprotonated species and 13 as the neutral species. Eq 14a has treated compound 13 as the protonated species (and 12 as the diprotonated species). A possible rationale for treating compound 12 as the diprotonated species ($K_{\text{DNA}} 56.2 \cdot 10^4 \text{ M}^{-1}$) is that compound 10 which only differs from 12 by a $-\text{CH}_3$ substituent at position 9 on the acridine ring has a $K_{\text{DNA}} 3.3 \cdot 10^4 \text{ M}^{-1}$. The substantial difference in K_{DNA} appears at first sight unlikely to be solely due to the 9-methyl group substituent.

The observed K_{DNA} equilibrium constants are almost certainly a composite apparent constant comprised of several independent constants. From first principle and based on other observations of protein binding processes^{33,35,25,38} [Fong 2014-16] it is expected that some degree of desolvation of water molecules must occur before the acridine or acridine-like TPZ analogues can intercalate into the DNA (which also presumably requires some desolvation to accommodate the acridine ring). Lipophilicity or hydrophobic bonding would also be an important interaction during the intercalation process. It is noted that the side chain of DACA lies in the major groove, such that the long axis of DACA is aligned with the long axis of the DNA base pairs. It was found that the optimised structures of the TPZ analogues in water in this study were closely consistent with the configuration observed in the DACA x-ray structures.

The calculated binding energies of the {DNA-TPZ analogues} complexes are consistent with the equations 14 and 14(a) which show that binding of the TPZ analogues to DNA are mainly driven by desolvation and lipophilicity interactions of the protonated species. The DFT modelling of binding energies shows that desolvation of the of the TPZA analogues and the DNA moiety are the dominant drivers and that the N-protonated acridine analogues are more strongly bound to the DNA moiety in vacuo, but when desolvation is taken into account in the thermochemical cycle, the neutral species are more strongly intercalated with the two guanine nucleobases. However, they truncated model is not fully representative of DNA binding to the TPZ analogues, since it mainly calculates the intercalating binding of a small portion of a single helix, whereas the full DNA has two helices which have numerous solvation sites, and the polar TPZ moiety itself is not included. The diprotonated TPZ12 analogue complex with the DNA moiety does clearly show that diprotonation enhances

binding over that of just the intercalated mono-protonated TPZ analogue, which can be an important process in binding equilibria as measured by eq 14 and 14(a). These data do support the notion proposed in Hay's work that attaching substituents to TPZ that can complex (intercalate) with DNA in both neutral and protonated forms, thereby increasing the likelihood to DNA degradation and cellular cytotoxicity. It is clear that drug designing efforts aimed at enhancing TPZ anti-cancer efficacy must consider the impacts of desolvation and lipophilicity.

4.7 DFT modelling of TPZ@CB[7]

CB have been shown to confer increased stability to encapsulated drugs possibly by protecting the drug from reactive species during delivery, including blood plasma protein binding, and oral drug administration is also feasible for some drugs, eg cisplatin@CB[7]. CB[7] is the optimum sized CB for many drugs, and the increased solubility and bioavailability of many drug@CB[7] complexes is also an advantage. Cellular uptake of several CB[7] complexes has been demonstrated (possibly by macrophages) so the possibility of intracellular as well as extracellular drug delivery may be possible under certain circumstances. However it is expected that extracellular drug delivery would predominate, since drugs bind with CB in a dynamic reversible equilibrium so the release of the encapsulated drug occurs "by itself" driven by the dissolution and the associated dilution effect. The timescale of release can vary from minutes to hours for various complexes. CB also favour the binding of protonated forms of drugs, known as pK_a shifts, that may be relevant in tumours where the pH is usually slightly acidic.^{30,32} [Saleh 2013, Walker 2011]

The modelling results of this study suggest that a TPZ@CB[7] complex may be quite stable, and that release of the TPZ from the complex is also feasible. A TPZ@CB[7] could offer an alternative drug delivery vehicle approach to the conventional structure activity approach to improving drug transport and efficacy.

5. Conclusions

Using the multiparameter model (desolvation, lipophilicity, dipole moment, and molecular volume and/or adiabatic electron affinity) as per general equation 1, which has been shown to apply to a wide range of other biological processes, it is found that the model applies to the diffusion, antiproliferative assays IC_{50} and aerobic and hypoxic clonogenic assays for a wide range of TPZ analogues in MCL. The neutral and radical anion forms of the TPZ analogues have been investigated to find the dominant factors which dictate behaviour under aerobic and hypoxic conditions. Extravascular diffusion is governed by the desolvation, lipophilicity, dipole moment and molecular volume, similar to passive and facilitated permeation through the blood brain barrier and other cellular membranes. Hypoxic assay properties of the TPZ analogues show dependencies on the electron affinity, as well as lipophilicity and dipole moment and desolvation, similar to other biological processes involving permeation of cellular membranes, including nuclear membranes. Aerobic properties are dependent on the almost exclusively on the electron affinity, consistent with electron transfer involving free radicals being dominant with little or no drug permeation of membranes and most likely occurring in the ECM. As MCL are known to be an effective model of the extravascular compartment for solid tumours, these results have design implications for possibly enhancing the anti-cancer efficacy of TPZ analogues.

It has also been shown that a strong linear relationship exist between the adiabatic electron affinities and reduction potential in water of these TPZ analogues measured by pulse radiolysis. Similarly the calculated lipophilicity measure, $\Delta G_{lipo,CDS}$, and the experimental

water-n-octanol partition coefficients, log P, are well correlated, despite the known problems with such partitioning experiments.

From an examination of the application of the general equation 1 to the DNA binding equilibrium constants of a series of TPZ analogues with acridine or acridine-like moieties, it is concluded that ligand water desolvation and lipophilicity are the dominant processes governing the DNA intercalation of TPZ analogues. DFT modelling of the complexes formed by TPZ analogues with neutral and N-protonated acridine moieties which intercalate with the guanine DNA nucleobases is also consistent with the results from applying equation 1 to measured equilibrium constants.

The correlations allow changes in the molecular structures of TPZ analogues to be made by drug designers and consequent integrated prediction of drug transport, antiproliferation, aerobic and hypoxic efficacy.

DFT QM modelling has shown that TPZ should form stable inclusion complexes with CB[7] and would be expected to dynamically release TPZ in aqueous environments.

Funding sources:

This research did not receive any specific grant from funding agencies in the public, commercial, or not-for-profit sectors.

References

- [1] Vaupel P. (2008) Hypoxia and aggressive tumor phenotype: implications for therapy and prognosis. *Oncologist* Vol. 13, (Suppl 3) pp.21–26.
- [2] Vaupel P. (2010). Metabolic microenvironment of tumor cells: a key factor in malignant progression. *Exp Oncol.* Vol. 32, pp.125–127.
- [3] Vaupel P, Kelleher DK. (2013) Blood flow and oxygenation status of prostate cancers. *Adv Exp Med Biol.* Vol. 765, pp. 299–305.
- [4] Tredan O, Galmarini CM, Patel K, Tannock IF. (2007) Drug Resistance and the Solid Tumor Microenvironment. *J Natl Cancer Inst.* Vol. 99, pp.1441–54.
- [5] Minchinton AI, Tannock IF. (2006) Drug penetration in solid tumours. *Nature Reviews Cancer*, Vol. 6, pp.583-592.
- [6] Muz B, de la Puente P, Azab F, Azab AK. (2015) The role of hypoxia in cancer progression, angiogenesis, metastasis, and resistance to therapy. *Hypoxia*, Vol. 3, pp. 83–92
- [7] Pettersen EO, Ebbesen P, Gieling RG, Williams KJ, et al. (2014) Targeting tumour hypoxia to prevent cancer metastasis. From biology, biosensing and technology to drug development: the METOXIA consortium. *J Enzyme Inhib Med Chem.* pp.1–33 DOI: 10.3109/14756366.2014.966704
- [8] Wardman P. Chemical radiosensitizers for use in radiotherapy, (2007) *Clinical Oncology*, Vol. 19, pp. 397-417.
- [9] von Sonntag C. (2006) *The oxygen effect, chemical repair and sensitization. Free-Radical-Induced DNA Damage and Its Repair: A Chemical Perspective*, Springer Ch 12.12.
- [10] Evans JW, Yudoh K, Delahoussaye YM, Brown JM. (1998) Tirapazamine is metabolized to its DNA-damaging radical by intranuclear enzymes. *Cancer Research.* Vol. 58, pp.2098-2101.

- [11] Junnotula V, Sarkar U, Sinha S, Gates K. Initiation of DNA strand cleavage by 1,2,4-benzotriazine 1,4-dioxide antitumor agents: mechanistic insight from studies of 3-methyl-1,2,4-benzotriazine 1,4-dioxide. (2009) *J Am Chem Soc.* Vol.131 (13), pp. 1015–24.
- [12] Brown, M. Wilson, W. (2004) Exploiting tumour hypoxia in cancer treatment. *Nature Reviews Cancer.* Vol. 4 (6), pp. 437–447.
- [13] Yin J, Glaser R, Gates KS. (2012) Electron and Spin-Density Analysis of Tirapazamine Reduction Chemistry. *Chem Res Toxicol.* Vol. 25, pp.620–633.
- [14] Shen X, Rajapakse A, Gallazzi F, Junnotula V, Fuchs-Knotts T, Glaser R, Gates KS. (2014) Isotopic labeling experiments that elucidate the mechanism of DNA strand cleavage by the hypoxia-selective antitumor agent 1,2,4-benzotriazine 1,4-di-*N*-oxide, *Chem Res Toxicol.* Vol. 27(1), pp. 111–118.
- [15] Rowinsky EK. (1999) Novel radiation sensitizers targeting tissue hypoxia. *Oncology.* Vol. 13(Suppl 5), pp. 61-70.
- [16] Green JA. (2016) Hypoxic cell sensitization in chemoradiation for cervical cancer. *Transl Cancer Res.* Vol. 5, pp.196-198.
- [17] DiSilvestro PA, Ali S, Craighead PS, Lucci JV, Lee Y, et al. (2014) Phase III Randomized Trial of Weekly Cisplatin and Irradiation Versus Cisplatin and Tirapazamine and Irradiation in Stages IB2, IIA, IIB, IIIB, and IVA Cervical Carcinoma Limited to the Pelvis: A Gynecologic Oncology Group Study. *J Clinical Oncology,* Vol. 32, pp.458-464.
- [18] Rischin D, Peters LJ, O'Sullivan B, Giralt Fisher JR, et al. (2010) Tirapazamine, Cisplatin, and Radiation Versus Cisplatin and Radiation for Advanced Squamous Cell Carcinoma of the Head and Neck (TROG 02.02, HeadSTART): A Phase III Trial of the Trans-Tasman Radiation Oncology Group. *J Clinical Oncology,* Vol. 28, pp. 2989-2995.
- [19] Kovacs MS, Hocking DJ, Evans JW, Siim BG, Wouters BG, Brown JM. (1999) Cisplatin anti-tumour potentiation by tirapazamine results from a hypoxia-dependent cellular sensitization to cisplatin. *Brit J Cancer,* Vol. 80, pp.1245–1251.
- [20] Denny WA, Wilson WR. (2000) Tirapazamine: a bioreductive anticancer drug that exploits tumour hypoxia. *Expert Opin Investig Drugs.* Vol. 9, pp. 2889–2901.
- [21] Hicks KO, Pruijn FB, Secomb TW, et al. (2006) Use of three-dimensional tissue cultures to model extravascular transport and predict in vivo activity of hypoxia-targeted anticancer drugs. *J. Natl. Cancer Inst.* Vol. 98, pp. 1118–1128.
- [22] Pruijn FB, Sturman JR, Liyanage HDS, Hicks KO, Hay MP, Wilson WR. (2005) Extravascular Transport of Drugs in Tumor Tissue: Effect of Lipophilicity on Diffusion of Tirapazamine Analogues in Multicellular Layer Cultures. *J Med Chem.* Vol. 48, pp. 1079-1087.
- [23] Pruijn FB, Patel K, Hay MP, Wilson WR, Hicks KO. (2008) Prediction of Tumour Tissue Diffusion Coefficients of Hypoxia-Activated Prodrugs from Physicochemical Parameters. *Aust J Chem.* Vol. 61, pp. 687–693.
- [24] (a) Hay MP, Gamage SA, Kovacs MS, Pruijn FB, Anderson RF, Patterson AV, et al. (2003) Structure-activity relationships of 1,2,4-benzotriazine 1,4-dioxides as hypoxia-selective analogues of tirapazamine. *J Med Chem.* Vol. 46, pp. 169-82. (b) Hay MP, Pruijn FB, Gamage SA, H. D. Liyanage S, Kovacs MS, Patterson AV, et al. (2004) DNA-Targeted 1,2,4-Benzotriazine 1,4-Dioxides: Potent Analogues of the Hypoxia-Selective Cytotoxin Tirapazamine. *J Med Chem.* Vol. 47, pp. 475-488.
- [25] Kyle AH, Minchinton AI. (1999) Measurement of delivery and metabolism of tirapazamine to tumour tissue using the multilayered cell culture model. *Cancer Chemotherap Pharmacol.* Vol. 43, pp. 213–220
- [26] Ljungkvist AS, Bussink J, Rijken PF, Kaanders JH, van der Kogel AJ, Denekamp J. (2002) Vascular architecture, hypoxia, and proliferation in first-generation xenografts of

- human head-and-neck squamous cell carcinomas. *Int J Radiat Biol Oncol Phys*. Vol. 54, pp. 215-28.
- [27] Walton MI, Workman P. (1993) Pharmacokinetics and bioreductive metabolism of the novel benzotriazine di-N-oxide hypoxic cell cytotoxin tirapazamine (WIN 59075; SR 4233; NSC 130181) in mice. *J Pharmacol Exp Ther*. Vol. 265, pp. 938-47.
- [28] Skarsgard LD, Skwarchuk MW, Vinczan A, Chaplin DJ. (1993) The effect of pH on the aerobic and hypoxic cytotoxicity of SR4233 in HT-29 cells. *Br J Cancer*, Vol. 68, pp. 681-683.
- [29] Agarwal S, Shankar RV, Inge LJ, Kodibagkar V. (2015) MRI assessment of changes in tumor oxygenation post hypoxia-targeted therapy. *Proc. SPIE 9417, Medical Imaging 2015: Biomedical Applications in Molecular, Structural, and Functional Imaging*, 941714, March 17, doi:10.1117/12.2083926
- [30] Saleh N, Ghosh I, Nau WM. (2013) Cucurbiturils in Drug Delivery And For Biomedical Applications, Chapter 7, p.164-212. *Cucurbiturils in Drug Delivery And For Biomedical Applications, Supramolecular Systems in Biomedical Fields*, Ed. Hans-Jörg Schneider, Royal Society of Chemistry.
- [31] Nau WM, Flore M, Assaf KI. (2011) Deep Inside Cucurbiturils: Physical Properties and Volumes of their Inner Cavity Determine the Hydrophobic Driving Force for Host–Guest Complexation. *Israel J Chem*. Vol. 51, pp. 559–577
- [32] Walker S, Oun R, McInnes FJ, Wheate NJ. (2011) The potential of cucurbit[n]urils in drug delivery. *Israel J Chem*. Vol. 51, pp. 616-624.
- [33] Fong CW. (2016) Drug discovery model using molecular orbital computations: tyrosine kinase inhibitors. *HAL Archives*, hal-01350862v1
- [34] Fong CW. (2015) Permeability of the Blood–Brain Barrier: Molecular Mechanism of Transport of Drugs and Physiologically Important Compounds. *J Membr Biol*. Vol. 248, pp. 651-69.
- [35] Fong CW. (2016) The effect of desolvation on the binding of inhibitors to HIV-1 protease and cyclin-dependent kinases: Causes of resistance. *Bioorg Med Chem Lett*. Vol. 26, pp. 3705–3713.
- [36] Fong CW. (2016) Predicting PARP inhibitory activity – A novel quantum mechanical based model. *HAL Archives*, hal-01367894v1.
- [37] Fong CW. (2016) A novel predictive model for the anti-bacterial, anti-malarial and hERG cardiac QT prolongation properties of fluoroquinolones. *HAL Archives*, hal-01363812v1.
- [38] CW Fong, (2016) Statins in therapy: Cellular transport, side effects, drug-drug interactions and cytotoxicity - the unrecognized role of lactones. *HAL Archives*, hal-01185910v1.
- [39] Fong CW. (2016) Physiology of ionophore transport of potassium and sodium ions across cell membranes: Valinomycin and 18-Crown-6 Ether. *Int J Comput Biol Drug Design*. Vol. 9, pp. 228-246.
- [40] Fong CW. (2016) Cucurbiturils as potential free radical chemoradiosensitizers for enhanced cisplatin treatment of cancers: A quantum mechanical study. *J Inklus Phenom Macro Chem*. In Press.
- [41] Marenich AV, Cramer CJ, Truhlar DJ. (2009) Universal Solvation Model Based on Solute Electron Density and on a Continuum Model of the Solvent Defined by the Bulk Dielectric Constant and Atomic Surface Tensions. *J Phys Chem B*, Vol.113, pp. 6378 -96
- [42] Rayne S, Forest K. (2010) Accuracy of computational solvation free energies for neutral and ionic compounds: Dependence on level of theory and solvent model. *Nature Proceedings*, <http://dx.doi.org/10.1038/npre.2010.4864.1>.

- [43] Rizzo RC, Aynechi T, Case DA, Kuntz ID. (2006) Estimation of Absolute Free Energies of Hydration Using Continuum Methods: Accuracy of Partial Charge Models and Optimization of Nonpolar Contributions. *J Chem Theory Comput.* Vol. 2, pp. 128-139.
- [44] Peverati R, Truhlar DG. (2014) The quest for a universal density functional: the accuracy of density functionals across a broad spectrum of databases in chemistry and physics. *Phil Trans Soc A*, 372, DOI: 10.1098/rsta.2012.0476
- [45] Rienstra-Kiracofe JC, Tschumper GS, Schaeffer HS III, Nandi S, Ellison GB. (2002) Atomic and molecular electron affinities: Photoelectron experiments and theoretical computations. *Chem. Rev.* Vol. 102, pp. 231-282.
- [46] Riley KE, Op't Holt T, Merz KM. (2007) Critical Assessment of the Performance of Density Functional Methods for Several Atomic and Molecular Properties. *J Chem Theory Comput.* Vol. 3, pp. 407-433.
- [47] Seiwert TY, Salama JK, Vokes EF. (2007) The concurrent chemoradiation paradigm—general principles. *Nature Clin. Pract. Oncol.* Vol. 4, pp. 86-100.
- [48] Cummins J, Boyd G, Macpherson JS, Wolf H, Smith G, Smyth JF, Jodrell DI. (2002) Factors influencing the cellular accumulation of SN-38 and camptothecin. *Cancer Chemother. Pharmacol.* Vol. 49, pp.194-200.
- [49] Inbaraj JJ, Motten AG, Chignell CF. (2003) Photochemical and photobiological studies of tirapazamine (SR 4233) and related quinoxaline 1,4-Di-N-oxide analogues. *Chem Res Toxicol.* Vol.16, pp. 164-70.
- [50] Daniels JS, Gates KS, Tronche C, Greenberg MM. (1998) Direct evidence for bimodal DNA damage induced by tirapazamine. *Chem Res Toxicol.* Vol. 11, pp.1254-7.
- [51] Brown JM. (1999) The hypoxic cell: a target for selective cancer therapy. *Cancer Res.* Vol. 59, pp. 5863-70.
- [52] Ho J, Coote ML, Cramer CJ, Truhlar DG. (2016) Organic Electrochemistry, p.229-259, 5th ed. O. Hammerich and B. Speiser, CRC Press, Boca Raton, Florida. ISBN: 978-1-42-008401-6
- [53] Ramalho TC, da Cunha EFF, de Alencastro RB. (2004) Theoretical study of adiabatic and vertical electron affinity of radiosensitizers in solution part 2: analogues of tirapazamine. *J Theor Comput Chem.* Vol. 3, pp.1-9.
- [54] Radzicka A, Wolfenden R. (1988) Comparing the polarities of the amino acids: side-chain distribution coefficients between the vapor phase, cyclohexane, 1-octanol, and neutral aqueous solution. *Biochemistry.* Vol. 27, pp. 1664-1670
- [55] Lomize AL, Reibarkh MY, Pogozeva ID (2002). Interatomic potentials and solvation parameters from protein engineering data for buried residues. *Protein Science.* Vol,11 (8), pp. 1984-2000.
- [56] Braumann T. (1986) Determination of hydrophobic parameters by reverse-phase liquid chromatography: theory, experimental techniques and applications in studies on quantitative structure-activity relationships. *J Chromatogr.* Vol. 373, pp. 191-225
- [57] Dearden J.C. Bresnen G.M. (1988) The measurement of partition coefficients. *Quant Struct Activ Rel.* Vol.7, pp.133-144.
- [58] Todd AK, Adams A, Thorpe JH, Denny WA, Wakelin LPG, Cardin CJ. (1999) Major Groove Binding and 'DNA-Induced' Fit in the Intercalation of a Derivative of the Mixed Topoisomerase I/II Poison *N*-(2-(Dimethylamino)ethyl)acridine-4-carboxamide (DACA) into DNA: X-ray Structure Complexed to d(CG(5-BrU)ACG)₂ at 1.3-Å Resolution. *J Med Chem.* Vol. 42, pp. 536-540.
- [59] Roy D, Marianski M, Neepa I, Maitra MT, Dannenberg JJ. (2012) Comparison of some dispersion-corrected and traditional functional with CCSD(T) and MP2 ab initio methods:

Table 1. Properties of TPZ analogues

Hay 2003 Figures 1 & 2	Neutral Species TPZ Analogues				Radical Anion Species TPZ Analogues				
	CDS _{water} kcal/mol	CDS _{octane} kcal/mol	Dipole Moment Water D	Molecular Volume Water cm ³ /mol	CDS _{water} kcal/mol	CDS _{octane} kcal/mol	Dipole Moment Water D	Molecular Volume Water cm ³ /mol	Adiabatic Electron Affinity Water eV
H	5.27	-6.19	3	115	5.01	-6.11	5	134	3.58
8NEt ₂	6.15	-7.52	5.7	174	5.85	-7.25	11.2	193	3.39
8NMe ₂	5.54	-6.75	4.4	138	5.1	-6.46	8.3	122	3.4
8OMe	6.31	-5.66	3.2	135	6.1	-5.54	5.5	146	3.55
8Me	5.41	-6.4	3.2	119	5.2	-6.23	5.35	144	3.47
8F	5.8	-5.62	4.1	122	5.6	-5.43	5.74	116	3.64
8Cl	5.19	-6.65	3.85	107	4.94	-6.4	5.23	126	3.65
8CF ₃	6.8	-5.29	5.5	124	6.6	-5.2	5.45	153	3.74
8SO ₂ Me	5.78	-6.14	7.4	141	5.6	-6.04	4.7	173	3.81
8SO ₂ Bu	6.3	-8.13	7.2	217	6.1	-8	7.1	245	3.8
7NMe ₂	5.6	-6.64	7.5	153	5	-6.5	11.4	133	3.44
7OMe	6.7	-5.77	3.4	146	6.4	-5.6	6.9	130	3.52
7Me	5.7	-6.47	4.14	122	5.5	-6.4	6.9	137	3.52
7F	5.91	-5.49	2.9	133	5.7	-5.4	4.8	132	3.66
7Cl	5.3	-6.5	2.73	142	5.1	-6.5	5.3	120	3.51
7CF ₃	7.2	-5.05	3.43	147	7	-4.96	5.8	165	3.33

7SO ₂ Me	6.2	-6.27	7.7	164	6	-6.13	7.07	165	3.79
7NO ₂	8.1	-6.52	12.8	153	8.2	-6.51	6.9	127	4.07
6NMe ₂	6	-6.51	9.8	146	4.9	-6.44	13.2	169	3.28
6OMe	6.7	-5.7	5.65	182	6.35	-5.6	9.35	147	3.49
6Me	5.73	-6.4	4.33	119	5.73	-6.4	6.38	141	3.5
6F	5.95	-5.44	1	119	5.73	-5.4	4.1	113	3.61
6Cl	5.3	-6.45	0.7	117	5.1	-6.4	5.1	139	3.66
6CF ₃	7.23	-5	1.3	129	7.23	-5	5.1	145	3.59
6SO ₂ Me	6.3	-6.3	5.8	143	6.1	-6.22	6.5	165	3.86
5NEt ₂	5.99	-7.37	5.87	177	5.72	-7.2	12.6	189	3.42
5NMe ₂	5.1	-7.37	11	145	5.4	-6.46	5.9	150	3.42
5OMe	6.3	-5.67	4.1	157	6	-5.53	7.8	131	3.56
5Cl	5.21	-6.55	2.35	123	5	-6.5	5.5	130	3.64
5F	5.8	-5.58	2.6	116	5.57	-5.45	5	120	3.65
Acridone	4.66	-6.73	9.4	167	4.56	-6.73	11.52	148	
Mannitol	4.82	-3.37	3.1	127	4.84	-3.33	11.67	147	
Urea	3.43	-0.5	6.37	53	3.28	-0.16	5.57	53	
PII	7.03	-10.2	3.76	180	6.86	-10.16	5.22	174	
PIII	8.8	-10.8	4.45	208	8.61	-10.72	8.84	225	
Hicks									
2006									
Figure 2									
TPZ	5.2	-6.2	3.2	92	5	-6.1	5	134	3.58
#1 6Me	5.73	-6.42	4.4	136	5.5	-6.3	7.6	148	3.5
#2 7Cl	5.3	-6.6	2.7	102	5.3	-6.6	9.5	124	3.51
#3 8Cl	5.2	-6.6	3.8	128	5	-6.5	5.8	143	3.65
#4 7 SO ₂ Me	6.3	-6.4	7.8	160	6.1	-6.3	9	205	3.79
#5 Morph	3	-8.8	3.6	189	2.9	-8.56	11.6	198	3.59

#6 NPr ₂	5.4	-9.6	2.4	258	5	-9.3	15.2	232	3.59
#7	3.24	-7.9	3	199	3	-7.65	7.2	173	3.52
#8	3.5	-8	3.6	206	3	-7.66	7.5	181	3.53
#9 6OMe	4.15	-7.26	5.65	189	3.8	-7.65	7	221	3.5
#10 3Et	5.84	-5.63	5	122	5.7	-5.6	3.9	141	3.62
#11 3EtOMe	6.87	-5.5	5	145	6.7	-5.5	1.5	153	3.65
#12	6.7	-14.84	10.1	374	6.6	-14.6	34.5	347	3.52
#13	6	-15.23	14.3	405	5.83	-14.9	31.4	402	3.59
#14	6.6	-15.4	12.1	465	6.1	-15.1	32.2	325	3.6
#15	7.85	-16	13.1	451	7	-15.3	32.5	382	3.55